AD_____

Award Number: W81XWH-06-1-0381

TITLE: Role of Crk Adaptor Proteins in Cellular Migration and Invasion in Human Breast Cancer

PRINCIPAL INVESTIGATOR: Kelly E. Fathers

CONTRACTING ORGANIZATION: McGill University
Montreal, Quebec, Canada H3A 1A1

REPORT DATE: March 2009

TYPE OF REPORT: Annual Summary

PREPARED FOR: U.S. Army Medical Research and Materiel Command
Fort Detrick, Maryland 21702-5012

# REPORT DOCUMENTATION PAGE

*Form Approved*
*OMB No. 0704-0188*



| 1. REPORT DATE | 2. REPORT TYPE | 3. DATES COVERED |
|---|---|---|
| 01-03-2009 | Annual Summary | 1 Mar 2006 – 28 Feb 2009 |

**4. TITLE AND SUBTITLE**

Role of Crk Adaptor Proteins in Cellular Migration and Invasion in Human Breast Cancer

**5a. CONTRACT NUMBER**

**5b. GRANT NUMBER**
W81XWH-06-1-0381

**5c. PROGRAM ELEMENT NUMBER**

**6. AUTHOR(S)**

Kelly E. Fathers

Email: kelly.fathers@mail.mcgill.ca

**5d. PROJECT NUMBER**

**5e. TASK NUMBER**

**5f. WORK UNIT NUMBER**

**7. PERFORMING ORGANIZATION NAME(S) AND ADDRESS(ES)**

McGill University
Montreal, Quebec, Canada H3A 1A1

**8. PERFORMING ORGANIZATION REPORT NUMBER**

**9. SPONSORING / MONITORING AGENCY NAME(S) AND ADDRESS(ES)**
U.S. Army Medical Research and Materiel Command
Fort Detrick, Maryland 21702-5012

**10. SPONSOR/MONITOR'S ACRONYM(S)**

**11. SPONSOR/MONITOR'S REPORT NUMBER(S)**

**12. DISTRIBUTION / AVAILABILITY STATEMENT**
Approved for Public Release; Distribution Unlimited

**13. SUPPLEMENTARY NOTES**
Original contains colored plates: ALL DTIC reproductions will be in black and white.

**14. ABSTRACT** The Crk adaptor proteins (CrkI, CrkII and CrkL) play an important role during cellular signalling by mediating the formation of protein complexes. We examined how the loss of Crk would affect tumor progression using RNA interference, as well as examining the consequences of Crk over-expression. For each cancer cell line tested, loss of Crk expression corresponded with a significant decrease in cell migration, invasion, and adhesion, demonstrating that Crk adaptor proteins play an important role in integrating signals of highly malignant cancer cell lines. To formally test this in vivo, Crk was down-regulated using shRNA in breast cancer cells that have a high propensity to form bone metastases. Loss of Crk was associated with a significant decrease in the formation of bone metastases, as well as growth at both the primary and secondary sites. Loss of Crk was also associated with decreases in Rac and Cdc42 activation. These data demonstrate that Crk adaptor proteins play a role in breast cancer progression, however whether Crk proteins can lead to breast cancer development has not been addressed. To test this, transgenic mice over-expressing Crk in the mammary epithelium were established. Transgenic CrkI and CrkII mice undergoing puberty were found to have delayed ductal outgrowth. In post-pubertal CrkII mice, precocious ductal branching was observed, which was associated with enhanced proliferation. Focal mammary tumors or hyperplasias appeared in 18% of CrkII transgenic animals, with an average latency of 14 months. Thus, the present study demonstrates that the Crk adaptor proteins play an important role in integrating signals for mammary gland development and breast cancer progression.

**15. SUBJECT TERMS**
Breast cancer, migration, invasion, metastasis, adaptor proteins, mammary gland development, RNA interference, mouse models, progenitor cells, basal, luminal, epithelial, EMT

| 16. SECURITY CLASSIFICATION OF: | | | 17. LIMITATION OF ABSTRACT | 18. NUMBER OF PAGES | 19a. NAME OF RESPONSIBLE PERSON |
|---|---|---|---|---|---|
| a. REPORT | b. ABSTRACT | c. THIS PAGE | | | USAMRMC |
| U | U | U | UU | 55 | 19b. TELEPHONE NUMBER *(include area code)* |

## Table of Contents

***Role of Crk adaptor proteins in cellular migration & invasion in human breast cancer***

**Student: Kelly E. Fathers BC051116**

## INTRODUCTION

The Crk protein was originally identified as the oncogene fusion product of the CT10 chicken retrovirus (v-Crk) (1). Cellular homologues of v-Crk, include c-Crk, which encodes two alternatively spliced proteins (c-CrkI and c-CrkII), and c-CrkL. Crk proteins are composed of one Src homology 2 (SH2), and one or two Src homology 3 (SH3) domains (2). The Crk adaptor proteins (CrkI, CrkII and CrkL) play an important role during cellular signalling (of processes such as migration, invasion, & adhesion) by mediating the formation of protein complexes. Previous work in our lab has shown that the over-expression of Crk proteins promotes an invasive phenotype, regardless of upstream signalling implicating a role for Crk proteins in cancer (3, 4). Moreover, Crk proteins are over-expressed in multiple types of cancer, including lung carcinoma, glioblastoma, and breast cancer (5, 6, 7). Although many studies have focused on the over-expression of Crk being important for many cellular processes, their significance in inherently motile cancer cells still remains elusive. Furthermore, much of what has been proposed about Crk proteins in epithelial cells is based upon *in vitro* over-expression studies or the use of dominant interfering mutants of CrkI/II or CrkL. These approaches, while informative, are limited by the challenges intrinsic to over-expression systems and these *in vitro* assays do not truly reflect the complexity of an *in vivo* response. Thus, the goal of our study was to examine if Crk adaptor proteins are truly responsible for mediating signals required for migration and invasion by validating how loss of Crk would affect these processes. Through the use of short interfering RNA (siRNA) silencing techniques and *in vivo* model systems, I will establish experimental models to formally test the hypothesis that *Crk proteins play an important role in cellular migration, invasion and metastasis, through their ability to recruit specific protein-protein complexes.* Our study on Crk adaptor proteins has the potential to identify some of the molecular events, which can occur during metastasis. Furthermore, since Crk proteins are over-expressed in human breast cancer, I will establish mouse models to test the hypothesis that *over-expression of Crk can promote breast tumorigenesis.* This may provide information, which could be used to develop effective treatments for breast cancer.

**BODY:**

**(1) Role of Crk in cellular migration and invasion in various types of cancer**

Several studies have suggested that Crk mediates cellular migration and invasion downstream of various stimuli. *I tested the hypothesis that Crk functions as a central adaptor protein that integrates upstream signals for cell migration and invasion by examining how the loss of Crk expression affects these processes in highly invasive cancer cell lines*. Using RNAi, I targeted CrkI, CrkII and CrkL in highly malignant breast cancer cell lines (MDA-435s and MDA-231) and found that the loss of Crk was associated with a decrease in cellular invasion and migration (7). These results demonstrate that Crk adaptor proteins play an important role in the promotion of signals for cell migration and invasion in human breast cancer cell lines irrespective of the upstream regulatory events that promote the invasive response. These results are now published in Molecular Cancer Research (7).

**(2) Role of Crk adaptor proteins in metastasis**

We previously demonstrated in the first objective that loss of CrkI/II results in decreased cellular migration, invasion and adhesion of various cancer cell lines, demonstrating that CrkI/II proteins are key integrators for these processes. This information identifies a potential role for Crk in metastasis since metastatic cells must possess all the necessary capabilities to efficiently complete the metastatic cascade, including: migratory, invasive, proteolytic, pro-survival, pro-coagulant, and pro-angiogenic properties. The conclusion that Crk adaptor proteins regulate migration and invasion in highly aggressive cancer cells *in vitro*, coupled with the knowledge that elevated levels of CrkI/II proteins are observed in human breast cancer, highlights the fact that the precise role of Crk in breast cancer metastasis still needs to be addressed. *I hypothesize that Crk proteins play a critical role in the metastatic spread of human breast tumors.* To test this hypothesis, I utilized both cell-based studies and animal models to better understand the role of Crk in the metastatic cascade.

Breast cancer metastasizes preferentially to bone, liver, brain and lung. Of the breast cancer patients who die from metastatic disease, 90% of them have bone metastases. Kang and colleagues derived a subpopulation of breast cancer cells (MDA-231 1833TR) with a higher affinity to form bone metastases to identify the molecular mechanisms required for metastasis (8). Since we identified Crk adaptor proteins as being important regulators of processes

necessary for successful metastasis in the parental population of these breast cancer cells *in vitro*, in this next objective, we tested the hypothesis that Crk plays a role in the metastatic process *in vivo*. To test this, we examined whether loss of Crk proteins could decrease the formation of bone metastases in this highly metastatic breast cancer cell line.

We generated stable knockdown of Crk (CrkI/CrkII/CrkL) using a shRNA mediated approach in MDA-231 1833TR breast cancer cell lines. Loss of Crk did not significantly impact cellular proliferation or anchorage independent growth in the presence of serum, albeit loss of Crk did impair the ability of breast cancer cells to grow in soft agar under quiescent conditions. In addition, Crk knockdown decreased the migratory and invasive capabilities of these highly metastatic cells as well as their ability to form invadopodia, which are actin-rich structures believed to be important in cellular invasion. Crk knockdown was associated with a decrease in the formation of bone metastases, with both the number and size of osteolytic lesions decreased in the Crk knockdown cells compared to the control cells. Moreover, loss of Crk inhibited growth at both the primary and secondary site. Crk knockdown was associated with decreased phosphorylation of p130Cas, and decreases in Cdc42 and Rac1 activation. Thus, the Crk adaptor proteins act as key signaling integrators for breast cancer metastasis to bone, facilitating our understanding of this process *in vivo*. The data is provided in Appendix 1 which contains all figures and figure legends.

**(3) To examine Crk dependent signaling pathways involved in cancer cell migration and invasion**

In this study, I utilized microarray analysis to gain insight into the Crk dependent molecular mechanisms involved in breast cancer progression. Over-expression of Crk can lead to the activation of various transcriptional pathways (AP-1, SRE-1) and Crk is a known activator of JNK and Rac, which can induce transcription (9, 10). Microarray analysis allowed me to identify the extent to which Crk is required for the regulation of genes involved in cancer promoting pathways and hence, determine the specific signals mediated by Crk. Breast cancer cell lines whose cellular migration and invasion are Crk dependent (i.e. MDA-231TR) were transiently transfected with non-targeting siRNA, Crk siRNA, CrkL siRNA, or combinations of the two (Crk, CrkL) and subjected to array analysis. A major advantage of this system, which distinguishes it from previous knockout approaches, is that the cells do not have to grow for long

periods without Crk, and will thus, not have the opportunity to accumulate mutations or adjust expression levels of genes that might compensate for the loss of Crk. Multiple siRNAs will be used in this experiment to control for potential off-targeting effects caused by siRNA duplexes (11). In addition, the gene lists from this experiment were compared to microarray analysis carried out on the stable Crk knockdown MDA-231 1833TR cell lines (described above), thus, providing a smaller gene list that is consistent between two different array experiments.

Several common genes were found when a comparison was made between MDA-231 1833TR Crk shRNA expression profiles and MDA-231TR Crk siRNA expression profiles. Interestingly, the expression of DOCK11, PAK6, ARHGEF4 and ARHGEF30 were all down-regulated upon loss of Crk. DOCK11 is a member of the DOCK180 family of guanine nucleotide exchange factors and is an activator of Cdc42 (12). Although a role for DOCK11 has not been established in breast cancer, DOCK11 is a candidate prognostic marker to identify carcinoma in situ (CIS), a common precursor of testicular germ cell tumours (13). PAK6, which is an effector protein for Cdc42, is highly expressed in primary and metastatic prostate cancers relative to normal prostate tissue (14, 15). Although the precise characterization of ARHGEF4 and ARHGEF30 have not been described, their identification as guanine nucleotide exchange factors for Rho GTPases, suggest that they activate Rho GTPase proteins by exchanging bound GDP for GTP (16).

The above mentioned genes are of interest as Cdc42 and Rac are thought to be important for breast cancer progression. For example, high Cdc42 and Rac1 are observed in human breast cancer (16). Moreover, Rac1 is required for Ras-induced malignant transformation, and is highly expressed in malignant versus benign breast tissue (16). Thus, the potential down-regulation of DOCK11, PAK6, ARHGEF4 and ARHGEF30, coupled with the decreases in Cdc42 and Rac activation observed in Crk knockdown cells and the significant *in vivo* tumour inhibition we observe, implicates both Rac and Cdc42 as being important mediators of breast cancer progression.

Finally, expression profiles from both MDA-231 TR and MDA-231 1833TR data sets were entered into the KEGG pathway analysis program, in which genes have been categorized based on their molecular function and biological processes. Using KEGG, we found that several potential biological processes were altered upon loss of Crk adaptor proteins. Categories significantly affected by loss of Crk proteins included various metabolic pathways, cytokine-

cytokine receptor interactions, focal adhesions, adheren junctions, cell adhesion molecules and extracellular-matrix interactions. An additional pathway analysis program (GO) revealed similar molecular processes affected in Crk knockdown cells, such as actin binding and cytoskeletal protein binding. This data is consistent with the finding that there were alterations in several genes whose molecular functions are involved in potential Crk-dependent pathways, such as Abl, ezrin, radixin and several regulators of Rho GTPase activation, including DOCK2, DOCK10, DOCK11, ELMO1, as well as the Rho guanine nucleotide exchange factors ARHGEF3, ARHGEF4, ARHGEF5, and ARHGEF12. Knockdown of CrkI/II and CrkL mRNA were confirmed through real-time PCR and validation of additional genes is ongoing. Our data implies that loss of Crk adaptor proteins may affect breast cancer development and metastasis in a multi-factorial manner. Thus, in addition to altering cellular signalling (Objective 2), loss of Crk affects the expression of genes whose functions may be required for breast cancer progression. The data is provided in Appendix 1 which contains all figures and figure legends.

**(4) Role of Crk adaptor proteins in the development of breast cancer using transgenic mice**

To examine *the importance of Crk adaptor proteins in tumor progression*, I used a transgenic mouse model, in which Crk proteins are over-expressed in the mammary epithelium. I have created constructs for CrkI, CrkII and CrkL, which allows the over-expression of these proteins through the hormonally responsive MMTV promoter. At the present time, MMTV-CrkII transgenic mice have been characterized and a manuscript is in preparation. As these results have previously been described in the 2008 final report, a quick summary is provided. Transgenic mice undergoing puberty were found to have delayed ductal outgrowth, compared to their wildtype littermates. This indicated a delayed development of the mammary gland and was characterized by increased collagen surrounding the terminal end bud. The fat pad was eventually filled and in older mice, there was precocious ductal branching associated with increased proliferation. Focal mammary tumours appeared in a subset of animals examined with a latency of approximately 15 months. MMTV-CrkII tumours showed high levels of Crk protein as well as various cytokeratin markers characteristic of these tumour pathologies. This study provides the first demonstration of a potential role for the CrkII adaptor protein in integrating signals for mammary gland development and breast cancer progression *in vivo*, which has important implications for elevated CrkII observed in human cancer.

The MMTV-CrkI and MMTV-CrkLV5 mice have been generated and their characterization is ongoing. For the MMTV-CrkI transgenic mice, the virgin and multiparous cohorts have been established and I am currently examining how over-expression of CrkI affects puberty, pregnancy, lactation and involution. At the present time, we have found that over-expression of CrkI delays ductal outgrowth, similar to over-expression of CrkII. Crosses with ErbB2 transgenic mice have also been established and the study is ongoing. For the MMTV/CrkLV5 transgenic mouse model, the founder lines have been established and the virgin and multiparous cohorts are being established. No delay in ductal outgrowth is evident in these transgenic animals. See Appendix 2 for a summary of the various MMTV-Crk mouse models.

In conclusion, we demonstrate that over-expression of various Crk adaptor proteins is associated with altered mammary gland development and accelerated tumour development. Although the low incidence of tumours in our transgenic mouse model highlights the fact that Crk proteins are not strong oncogenes, the ability of CrkII to induce a branching phenotype during a normally quiescent state suggests that it plays an active role in proliferation and epithelial remodeling. This precocious development, combined with the fact that Crk proteins are downstream of several signaling proteins involved in breast cancer development, highlights the potential consequence of increased Crk proteins in the human disease.

**KEY RESEARCH ACCOMPLISHMENTS**

(1) Discovered that Crk adaptor proteins are required for the efficient metastasis of breast cancers to bone.

(2) Established that Crk adaptor proteins are required for the development of breast cancer through shRNA based studies and mammary fat pad injections.

(3) Identified Crk adaptor proteins are being important regulators for Cdc42 activation.

(4) Demonstrated that loss of Crk expression results in the decreases in gene expression of several genes, whose functions are required for various aspects of tumour progression.
(5) Established the role of Crk adaptor proteins in promoting tumour development. The creation of MMTV-based mouse models over-expressing the Crk adaptor proteins in the mouse mammary gland confirmed that these oncogenes are not very strong, but rather collaborate with additional genetic events to promote tumorigenesis.
(6) Over-expression of Crk adaptor proteins alter the delicate balance of mammary gland development, leading to delayed ductal outgrowth (MMTV/CrkI, MMTV/CrkII) and enhanced branching (MMTV/CrkII).

## REPORTABLE OUTCOMES

### Manuscripts

Fathers, KE, Rajadurai, CV, Monast, A, Zhao, H, Pepin, F, Mourskaia, A, Zuo, D, Siegel, P, Park, M. 2009. Crk adaptor proteins act as key signaling integrators for breast cancer metastasis. (Manuscript in preparation for May 2009 submission).

Fathers, KE, Monast, A, Rodrigues, SP, Zuo, D, Zhao, H, Chughtai, N, Vasudeva Murthy, I, Cardiff, R, Park, M. 2009. CrkII transgene leads to atypical mammary gland development and tumorigenesis. (Manuscript in preparation for April 2009 submission).

Rodrigues, SP^, Fathers, KE^, Chan, G, Zuo, D, Halwani, F, Meterissian, S, Park, M. 2005. CrkI/II function as key signalling nodes for migration and invasion of cancer cells. Molecular Cancer Research. 3 (4):183-94

^ - Both authors contributed equally to this work.

### Abstracts

Fathers KE, Monast A, Rodrigues S, Park M. CrkII trangene leads to abnormal mammary gland development and tumorigenesis. Era of Hope – Department of Defense Breast Cancer Research Program, June 25-28, 2008. Baltimore, Maryland, USA.

Fathers KE, Monast A, Rodrigues S, Park M. CrkII trangene leads to abnormal mammary gland development and tumorigenesis. Gordon Research Conference – Mammary Gland Biology, June 1-5, 2008. Il Ciocco, Barga, Italy.

Fathers KE, Monast A, Rodrigues S, Park M. Over-expression of CrkII leads to abnormal mammary gland development and a basal cancer phenotype. Mechanisms and Models of Cancer. August 8-12$^{th}$, 2007. La Jolla, California, USA

Fathers KE, Monast A, Rodrigues S, Park M. MMTV-CrkII mice display a defective ductal outgrowth phenotype in peripubertal mice. Gordon Research Conference - Mammary Gland Biology. May 28-June 2, 2006. Il Ciocco, Barga Italy.

Fathers, KE, Rodrigues S, Park M.Crk adaptor proteins play a key role in cellular migration and invasion in human cancer. Canadian Breast Cancer Research Alliance - Reasons for Hope. Fourth Scientific Conference. Montreal, Quebec May 5-8, 2006

Fathers, KE, Rodrigues S, Park M. Crk adaptor proteins play a key role in cellular migration and invasion in human cancer. American Society of Cellular Biology - Systems Integration in Directed Cell Motility. University of Washington, Seattle, WA. July 27-30, 2005

Rodrigues, SP, Fathers, KE, Chan, G, Park, M. Crk adaptor proteins play an essential role in cellular migration and invasion in multiple human cancer cell lines. Twentieth Annual Meeting on Oncogenes, 2004. Frederick, Maryland, USA.

**Presentations**

Fathers, KE. Crk adaptor proteins act as key signaling integrators in breast cancer development and metastasis. Metastasis and Angiogenesis Research Meeting. McGill University, Montreal, Canada.

Fathers, KE. Crk adaptor proteins act as key signaling integrators in breast cancer development and metastasis. Invited speaker – Dec 10th, 2008. University of Toronto, Toronto, Canada.

Fathers, KE. Crk adaptor proteins act as key signaling integrators in human breast cancer. Molecular Oncology Group Seminar Series. McGill University, Montreal, Canada.

**Animal Models**

MMTV-CrkLV5

MMTV-CrkII

MMTV-CrkI

**Cell Lines**

MDA-231 breast cancer cell lines stably expressing shRNA targeting CrkI/II and CrkL

**CONCLUSION**

Our data demonstrates that Crk adaptor proteins play an important role in integrating signals for migration and invasion of highly malignant human cancer cell lines, regardless of the upstream signals promoting these cellular processes. These results are important, as progression of cancer to an invasive, metastatic lesion is dependent, in part, on the deregulation of signaling pathways involved in migration and invasion. We have shown the significance of Crk adaptor proteins during tumour progression as well as metastasis, which is the rate-limiting factor in cancer treatment. This has important consequences, as Crk proteins are over-expressed in many types of cancer, including breast cancer. In addition, our work has identified several molecular mechanisms by which Crk regulates breast cancer progression. This may provide information, which could be a valuable tool for the design and implementation of a therapeutic drug for breast cancer and its metastases, which is both highly specific and efficient.

**“SO WHAT”**

Metastasis is a major cause of morbidity and mortality in human malignancies, and is the driving force behind the incessant pursuit of “anti-metastatic” and adjuvant therapies. For instance, patients with metastatic breast cancer have a median survival of only 2 to 3 years and

twenty percent of the patients who present with bone metastases have only a five year survival from the time of diagnosis (17). As a result, current therapies for metastatic breast cancer are aimed at improving palliative care rather than complete remission (17). Further progress in this field of research may be achieved through a better understanding of the various molecular processes defining the complexity and multi-step nature of tumor cell dissemination, otherwise known as the metastatic cascade. My research has shown that Crk adaptor proteins are key integrators of breast cancer development and metastasis.

In addition to identifying a novel role for Crk adaptor proteins in breast cancer metastasis, I have shown that CrkII is linked to the formation of hyperplasias and breast cancer. The low penetrance and low latency suggests that over-expression of CrkII may not drive tumor development, although we know Crk expression is required for tumor progression based on our shRNA experiments. Combining my recent data with the previous data from our lab, which showed that Crk can convert a non-invasive response to an invasive response, suggests that Crk may not necessarily need to be elevated to be important for tumor development. In reality, Crk may synergize with several upstream signals to drive tumor progression rather than driving tumor progression itself. For instance, I have shown that loss of Crk inhibits migration and invasion of several “basal” breast cancer cell lines, signifying that Crk may be a key signaling node for multiple tumors, regardless of their inherent mutations. As these “basal” breast tumors are triple negative (Her2, ER, PR negative), treatment options are limited. Thus, the data generated from this study has the potential to identify Crk adaptor proteins as valuable targets for these types of breast tumors.

## REFERENCES


1. Mayer, B.J., Hamaguchi, M. & Hanafusa, H. (1988). Nature, 332, 272-5.
2. Matsuda, M., Tanaka, S., Nagata, S., et al. (1992). Mol Cell Biol. 12, 3482-89.
3. Lamorte, L., Rodrigues, S., Naujokas, M. & Park, M. (2002). J Biol Chem, 277, 37904-11.
4. Lamorte, L., Royal, I., Naujokas, M. & Park, M. (2002). Mol Biol Cell, 13, 1449-61.
5. Miller, C.T., Chen, G., Gharib, T.G., et al. (2003). Oncogene, 22, 7950-7.
6. Nishihara, H., Tanaka, S., Tsuda et al. (2002). Cancer Lett, 180, 55-61.
7. Rodrigues, S.P., Fathers, K.E., Chan, G., et al. (2005). Mol Cancer Res. 3(4): 183-94.
8. Kang, Y., Siegel, P.M., Shu, et al. (2003). Cancer Cell. 3(6): 537-49.

9. Iwahara, T., Akagi, T., Shishido, T., & Hanafusa, H. (2003). Oncogene. 22(38): 5946-57.
10. Tanaka S, Ouchi T, Hanafusa H. (1997). PNAS. 94(6):2356-61.
11. Jackson, A.L., Bartz, S.R., Schelter, J., et al. (2003). Nat Biotechnol. 21(6):635-7
12. Lin Q, Yang W, Baird D, et al. (2006). JBC. 281: 35253-62.
13. Almstrup K, Leffers H, Lothe RA, et al. (2007). Int J Androl 2007. 30: 292-302
14. Kaur R, Yuan X, Lu ML, Balk SP. (2008). Prostate. 68: 1510-6.
15. Lee SR, Ramos SM, Ko A, et al. (2002). Mol Endo. 16: 85-99.
16. Tang Y, Olufemi L, Wang MT, Nie D. (2008). Front Biosci. 13: 759-76.
17. Ali, S.M., Harvey, H.A., Lipton, A. (2003). Clin Orthop Relat Res. 415 (Suppl): S132-7.

# Appendix 1

# Crk adaptor proteins act as key signaling nodes for breast cancer metastasis

Kelly E. Fathers, Charles V. Rajadurai, Anie Monast, Hong Zhao, Francois Pepin, Anna Mourskaia, Dongmei Zuo, Peter Siegel, and Morag Park

**Figure 1 – Knockdown of Crk alters cell morphology, anchorage independent growth and cellular migration and invasion.** Western blot analysis of whole cell lysates (MDA-231 1833TR) with an anti-CrkI/II or anti-CrkL sera revealed that the CrkI/II and CrkL shRNA constructs efficiently and specifically target its respective RNA. Actin protein levels were used as a loading control (A). Alamar blue assay of control and Crk shRNA cells demonstrated no differences in cellular proliferation over time (B). Soft agar assays under low serum conditions (0.5% FBS) revealed differences in the ability of Crk shRNA cells to grow under anchorage independent conditions, relative to control MDA-231 1833TR cells. Images were taken using Lumenera Infinity Analyze software (C). Control cells and Crk shRNA cells plated onto

fibronectin coated coverslips revealed gross differences in cell morphology. Cells were co-stained with  -Paxillin/Alexa Fluor 555 goat anti-mouse and Phalloidin-488 for the F-actin staining. Images were acquired using a Zeiss confocal microscope. Actin and paxillin images were acquired using a 63x objective. Scale bars represent 10  m (D). Both control cells and Crk shRNA cells were analysed for their migration and invasion capacity in the presence of serum, with the Crk shRNA showing decreased migration and invasion relative to control cells. Cells were seeded into modified boyden chambers in the presence or absence of matrigel and assayed over a 24 hour period. Cells remaining on bottom of the porous membrane were fixed in formalin phosphate, stained with 0.2% crystal violet, washed, and left to dry overnight. Bottom layers of each transwell were imaged in 5 separate fields for each cell line using a 10x objective in phase contrast. Image analysis of these assays was carried out using ImageScope software. A minimum of three experiments was performed. Error bars represent the standard error of the three experiments (E, F).

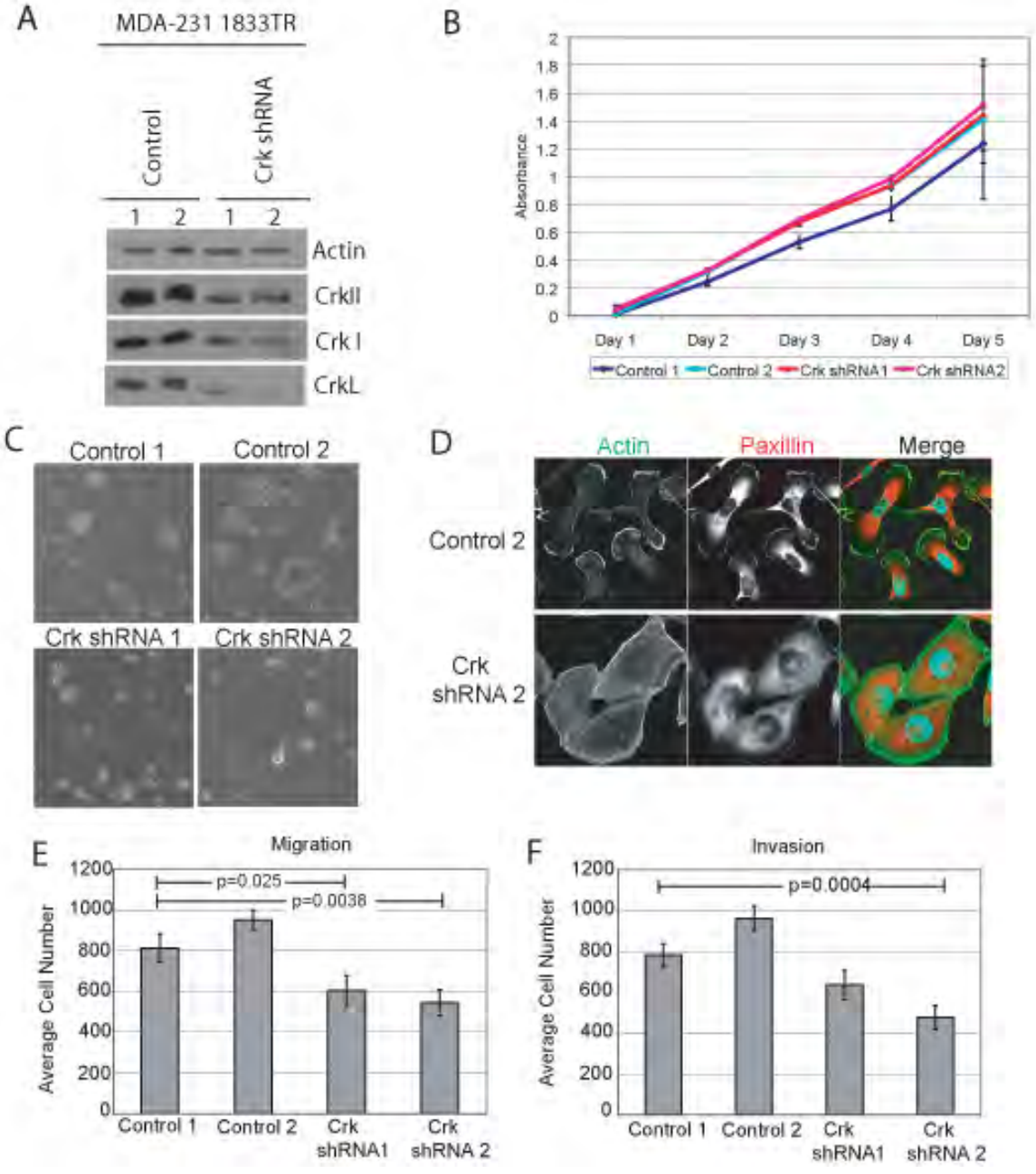
A
MDA-231 1833TR
Control
Crk shRNA
1 2 1 2
Actin
CrkII
Crk I
CrkL
B
Absorbance
Day 1
Day 2
Day 3
Day 4
Day 5
Control 1
Control 2
Crk shRNA1
Crk shRNA2
C
Control 1
Control 2
Crk shRNA 1
Crk shRNA 2
D
Actin
Paxillin
Merge
Control 2
Crk shRNA 2
E
Migration
Average Cell Number
p=0.025
p=0.0038
Control 1
Control 2
Crk shRNA1
Crk shRNA 2
F
Invasion
Average Cell Number
p=0.0004
Control 1
Control 2
Crk shRNA1
Crk shRNA 2

**Figure 2 - Crk adaptor proteins are required for efficient metastasis of breast cancer cells to bone.** MDA-231 1833TR control cells or those expressing Crk shRNA were injected into the left cardiac ventricle of female nude mice. Breast cancer cell outgrowth in bone was measured by bioluminescence imaging, which revealed less bioluminescence activity in Crk shRNA expressing cells compared to controls. A representative luciferase image at 40 days is shown, which closely resembles the mean bioluminescence values from each group (A). The whole body bioluminescence was quantified as the normalized photon flux (p/sec/cm2/sr) or relative luciferase units (RLU) over time. Averages from each cell line were plotted along with standard error (B). The bioluminescence derived from positive forelimbs and hindlimbs, which are the most common metastatic sites, were quantified in a similar manner to the whole body luminescence. Averages from each cell line were plotted along with standard error (C).

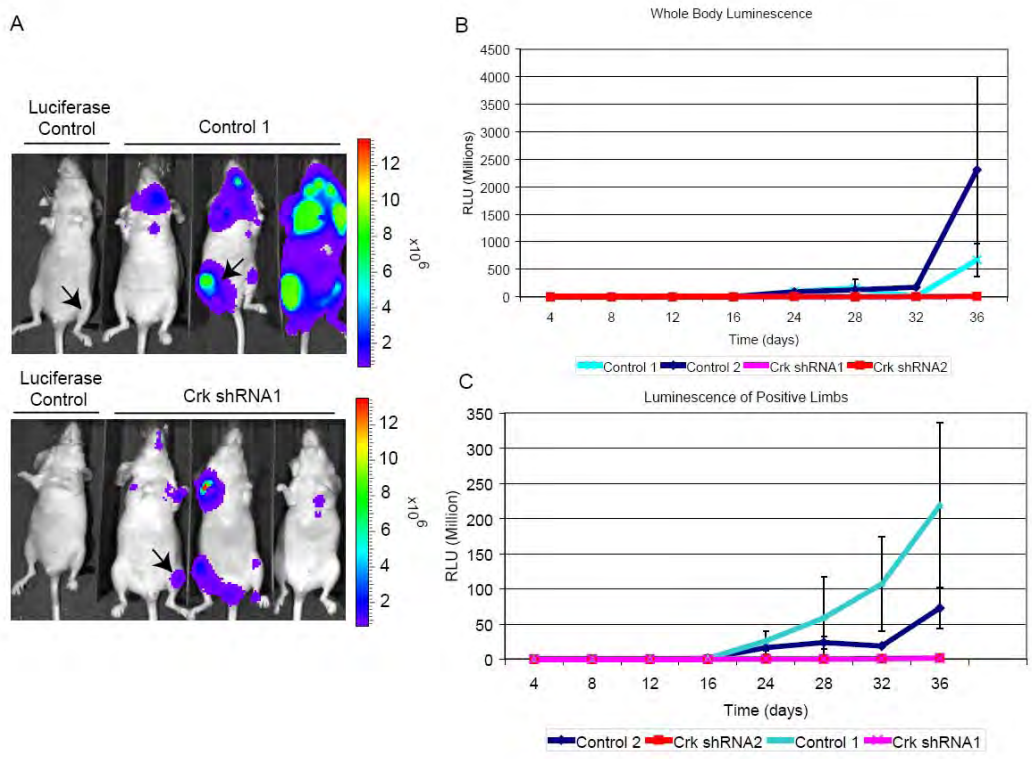

**Figure 3 - Crk adaptor proteins are required for the efficient osteolysis of bone.** MDA-231 1833TR control cells or those expressing Crk shRNA were injected into the left cardiac ventricle of female nude mice. Representative X-ray imaging of negative control mice, 1833TR control cells and Crk shRNA cells reveals a decrease in the number and size of osteolytic lesions in the Crk shRNA derived metastatic lesions (A). H&E stained tibial (control) and jaw (Crk shRNA) sections show similar pathology, however the intensity of CrkI/II and CrkL staining in Crk shRNA derived tumours is lower compared to control tumours. Images taken at 20x. Scale bar represents 50 μm (B). X-ray images of all the animals were first blinded and then scored for the number of osteolytic lesions for each condition. The average number of osteolytic lesions is decreased in the Crk shRNA derived metastases (C). X-ray images of all the animals were blinded and then scored for the average size of osteolytic lesions for each condition using ImageJ software. The average size of osteolytic lesions is decreased in the Crk shRNA derived metastases (D).

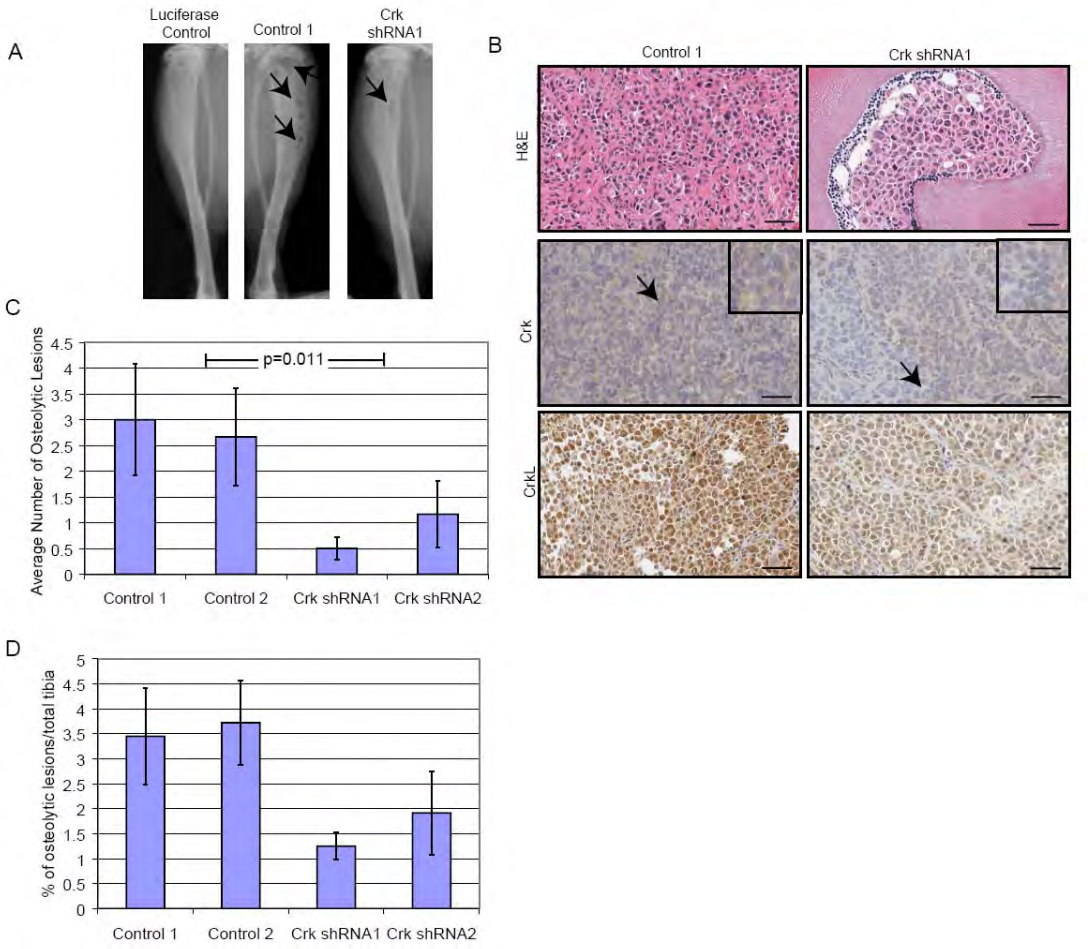

**Figure 4 - Crk knockdown affects the outgrowth of breast cancer cells within the bone.** MDA-231 1833TR control cells or those expressing Crk shRNA were injected directly into the tibia of female nude mice. Breast cancer cell outgrowth in the tibia was measured by bioluminescence imaging, which revealed less bioluminescence activity in the Crk shRNA expressing lesions compared to the controls. A representative luciferase image at 32 days is shown, which closely resembles the mean bioluminescence values from each group (A). The tibial outgrowth was quantified using only limbs positive for bioluminescent activity. It was measured as the normalized photon flux (p/sec/cm2/sr) over time, or relative luciferase units (RLU). Averages from each cell line were plotted along with standard error (B). Representative X-ray imaging of negative control mice, 1833TR control cells and Crk shRNA cells reveals a decrease in the number and size of osteolytic lesions in the Crk shRNA derived tibial outgrowths (C). X-ray images of all the animals were first blinded and then scored for the number of osteolytic lesions for each condition. The average number of osteolytic lesions is decreased in the Crk shRNA derived metastases (D). Blinded X-ray images of all the animals were also scored for the size of osteolytic lesions. The average size of osteolytic lesions is decreased in the Crk shRNA derived lesions (E). H&E stained sections show similar pathology. Paraffin embedded sections of tibial lesions derived from 1833TR control and Crk shRNA cells were stained for Ki67 and CrkL. Preliminary staining patterns revealed significant differences between the control and Crk knockdown tumours for Ki67 and CrkL staining intensity. All images taken at 20x where the scale bar represents 50 μm. Arrows represent positive staining (F).

**Figure 4**

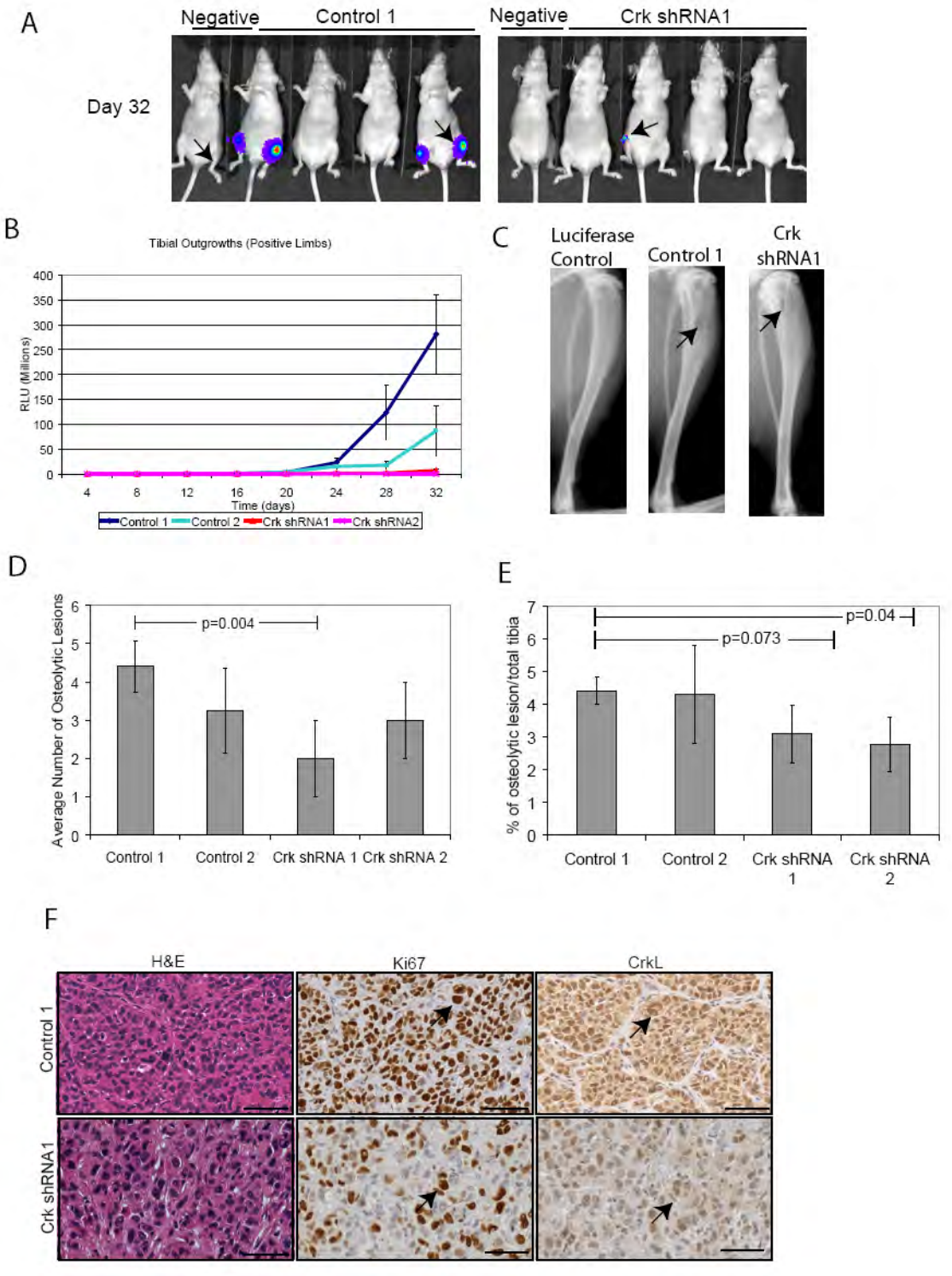
A
Negative
Control 1
Negative
Crk shRNA1
Day 32
B
Tibial Outgrowths (Positive Limbs)
RLU (Millions)
Time (days)
Control 1
Control 2
Crk shRNA1
Crk shRNA2
C
Luciferase Control
Control 1
Crk shRNA1
D
Average Number of Osteolytic Lesions
p=0.004
Control 1
Control 2
Crk shRNA 1
Crk shRNA 2
E
% of osteolytic lesion/total tibia
p=0.04
p=0.073
Control 1
Control 2
Crk shRNA 1
Crk shRNA 2
F
H&E
Ki67
CrkL
Control 1
Crk shRNA1

**Figure 5 – Crk adaptor proteins are essential for outgrowth in the primary site.** One million cells of either control 1833TR cells or Crk shRNA cells were injected into the fourth abdominal mammary fat pad of nude mice. Mammary tumour outgrowth was measured bi-weekly using caliper measurements, which revealed a longer latency of Crk shRNA derived tumours compared to the control cells. The average volume of control (n=10 per condition) and Crk shRNA tumours (n=8 per condition) were plotted over time along with standard error (A). H&E stained sections show similar pathology. Images taken at 20x. Scale bar represents 50 μm (B). Western blot analysis of Crk protein expression levels from cell lines prior to injection as well as tumour endpoint (C). Paraffin embedded sections of mammary tumours derived from 1833TR control and Crk shRNA cells were stained for Ki67 and TUNEL. Preliminary staining patterns revealed no significant differences between the control and Crk knockdown tumours for Ki67 and TUNEL. All images taken at 20x where the scale bar represents 50 μm. Arrows represent area of insert (D).

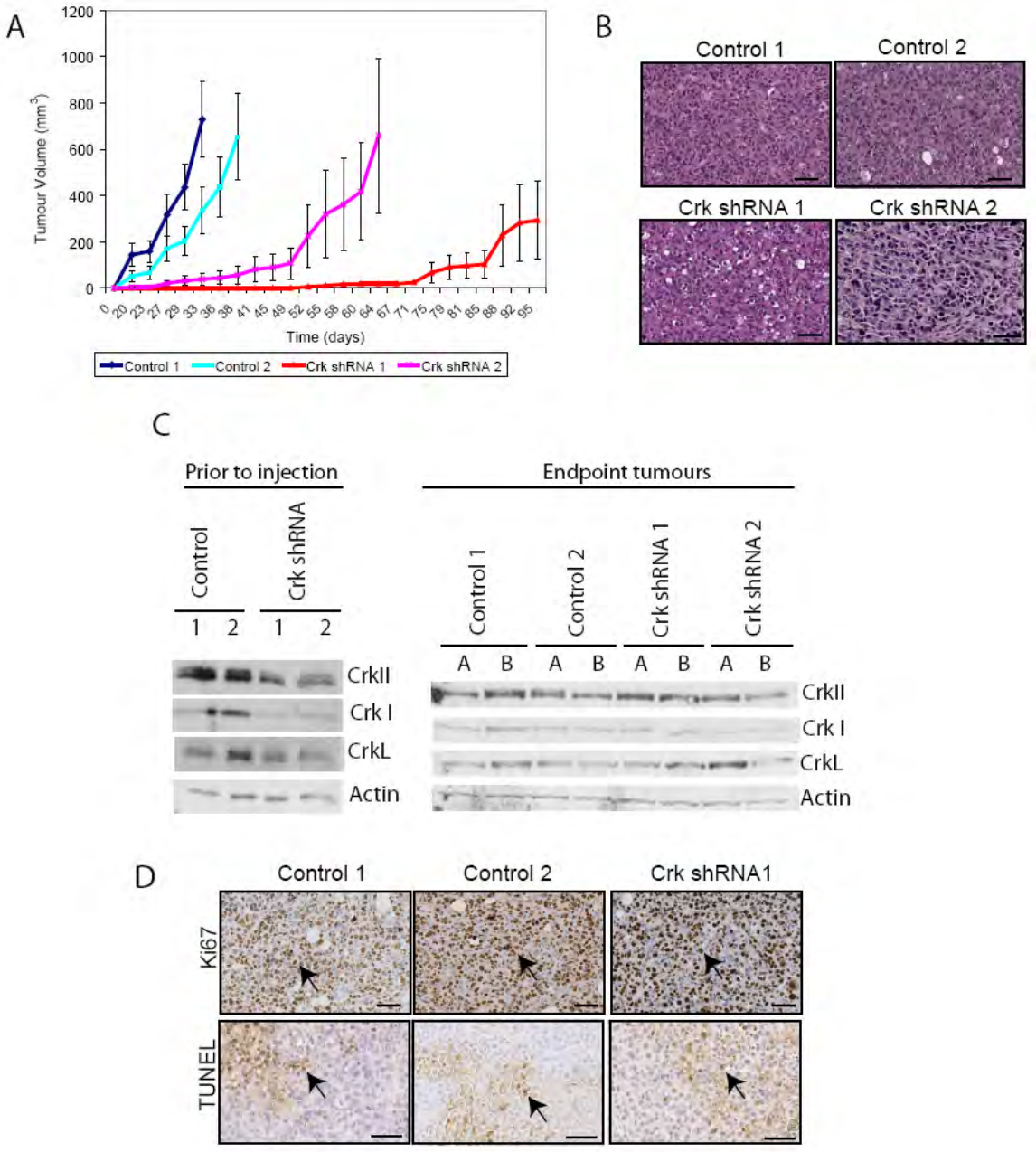
A
Tumour Volume (mm3)
Time (days)
Control 1
Control 2
Crk shRNA 1
Crk shRNA 2
B
Control 1
Control 2
Crk shRNA 1
Crk shRNA 2
C
Prior to injection
Endpoint tumours
Control
Crk shRNA
CrkII
Crk I
CrkL
Actin
D
Control 1
Control 2
Crk shRNA1
Ki67
TUNEL

**Figure 6 – Crk knockdown alters Cdc42 and Rac activation.** Western blot analysis of whole cell lysates (MDA-231 1833TR) with an anti-CrkI/II or anti-CrkL sera revealed that the CrkI/II and CrkL shRNA constructs efficiently and specifically target its respective RNA. Phosphorylation of p130Cas was decreased in Crk knockdown cells relative to the control cells, as determined by immunoblotting using whole cell lysates. No differences were seen in the phosphorylation levels of MAPK. Actin protein levels were used as a loading control (A). The GTP bound form of Rac was precipitated by GST-Pak-PBD and probed for anti-Rac1 sera. Total levels of Rac were visualized by immunoblotting (B). Activated levels of Rac1 were quantified by Image J analysis and compared to the total Rac1 levels and the ratio (activated/total Rac) was graphed. Three experiments were carried out and the average was plotted. The GTP bound form of Cdc42 was precipitated by GST-WASP and probed for anti-Cdc42 sera. Total levels of Cdc42 were visualized by immunoblotting (C). Activated levels of Cdc42 were quantified by Image J analysis as described above for Rac1.

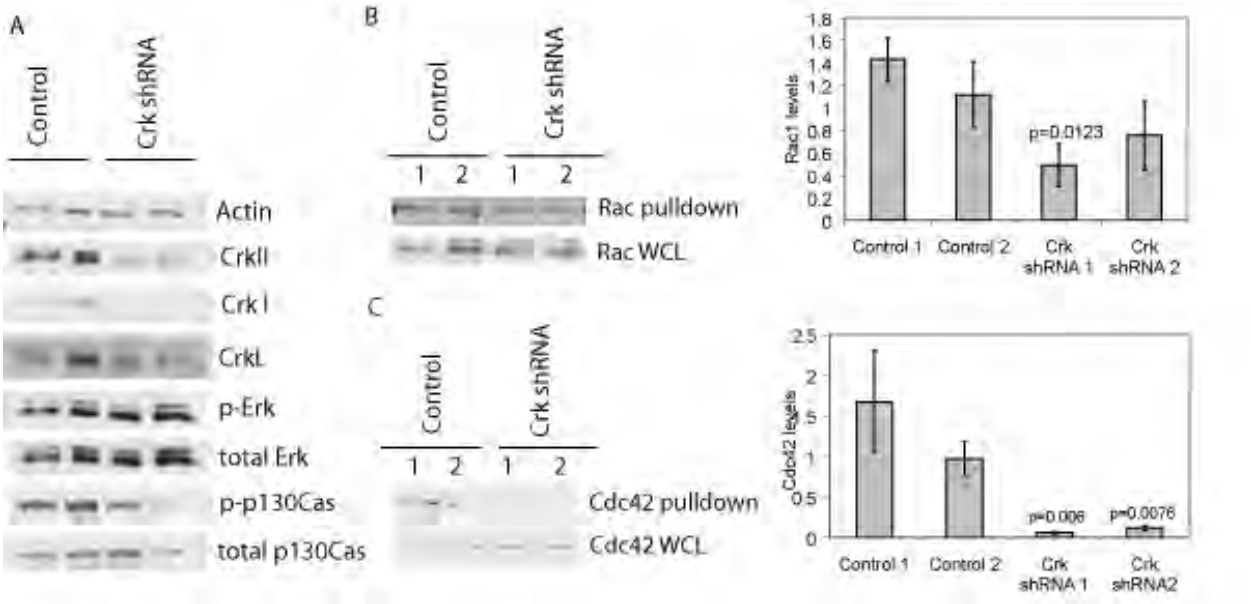

**Figure 7 – Crk knockdown in MDA231 1833TR cells results in changes in gene expression.** Hierarchical clustering of all stable cell lines reveal the control cell lines are more closely related to another than to the Crk knockdown cell lines and vice versa (A). Heatmap analysis demonstrates global changes in gene expression between control and Crk knockdown cell lines (B).

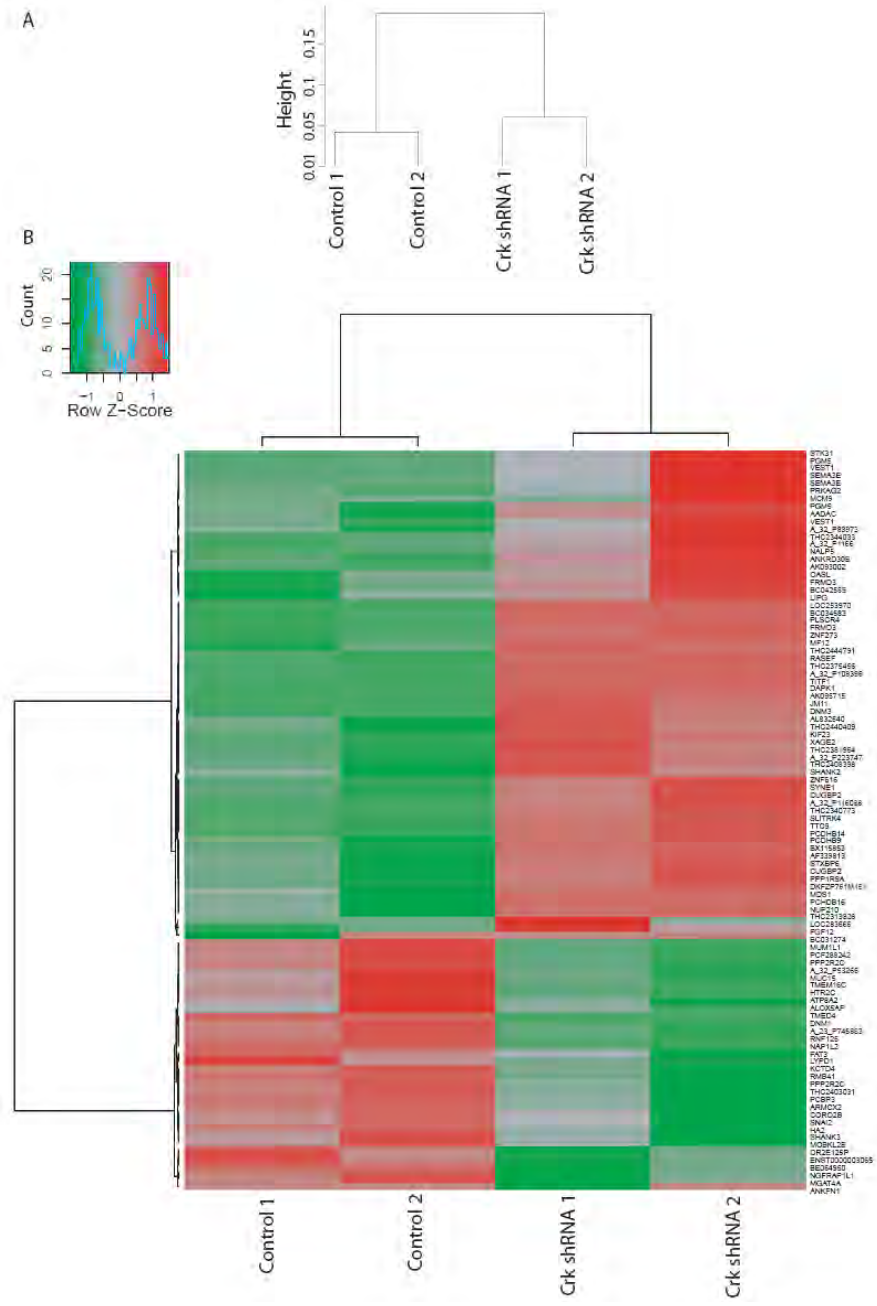

**Figure 8 – Crk knockdown results in changes in gene expression of genes whose functions are important for tumour progression.** KEGG pathway analysis demonstrates several different pathways up-regulated or down-regulated in Crk knockdown cells relative to control cell lines (A). Quantitative real-time PCR analysis identifies loss of CrkI/II and CrkL in Crk knockdown cells relative to control cells (B).

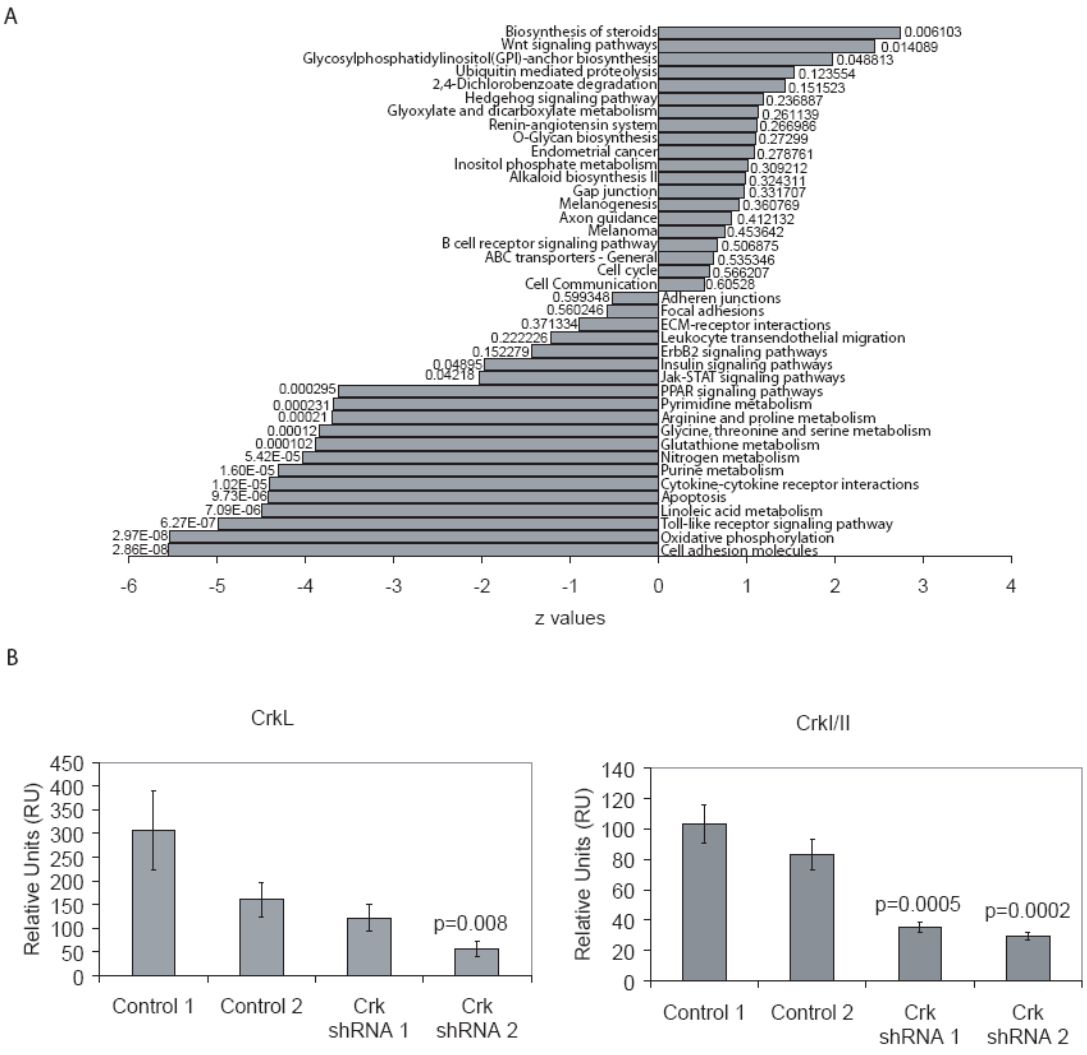

**Supplemental Figure 1 - Knockdown of Crk adaptor proteins does not affect anchorage independent growth when grown in serum.** Soft agar assays under normal, 10% serum revealed no differences in the ability of Crk shRNA cells to grow under anchorage independent conditions, relative to the control MDA-231 1833TR cells. Images were taken using the Axiovision software.

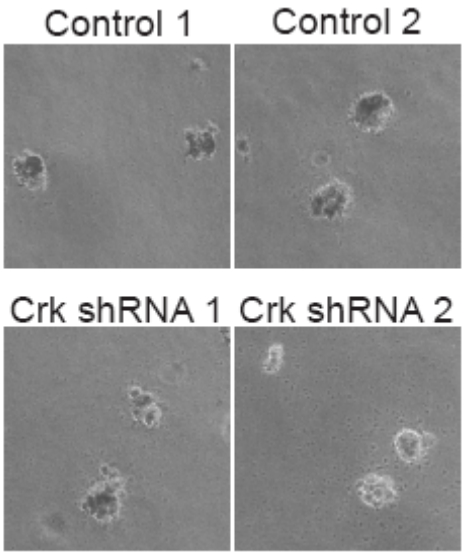

**Supplemental Figure 2 – Crk adaptor proteins are important regulators of invadopodia activity within 1833TR cells.** Control 1833TR cells and Crk shRNA cells were plated on FITC-labeled gelatin and the cells were examined for their ability to form actin-rich structures as well as degrade gelatin. The control cells formed prominent actin-rich structures believed to be invadopodia, and had the ability to degrade gelatin. The Crk shRNA cells still formed prominent actin rich structures, but had a significant impairment in their ability to degrade gelatin.

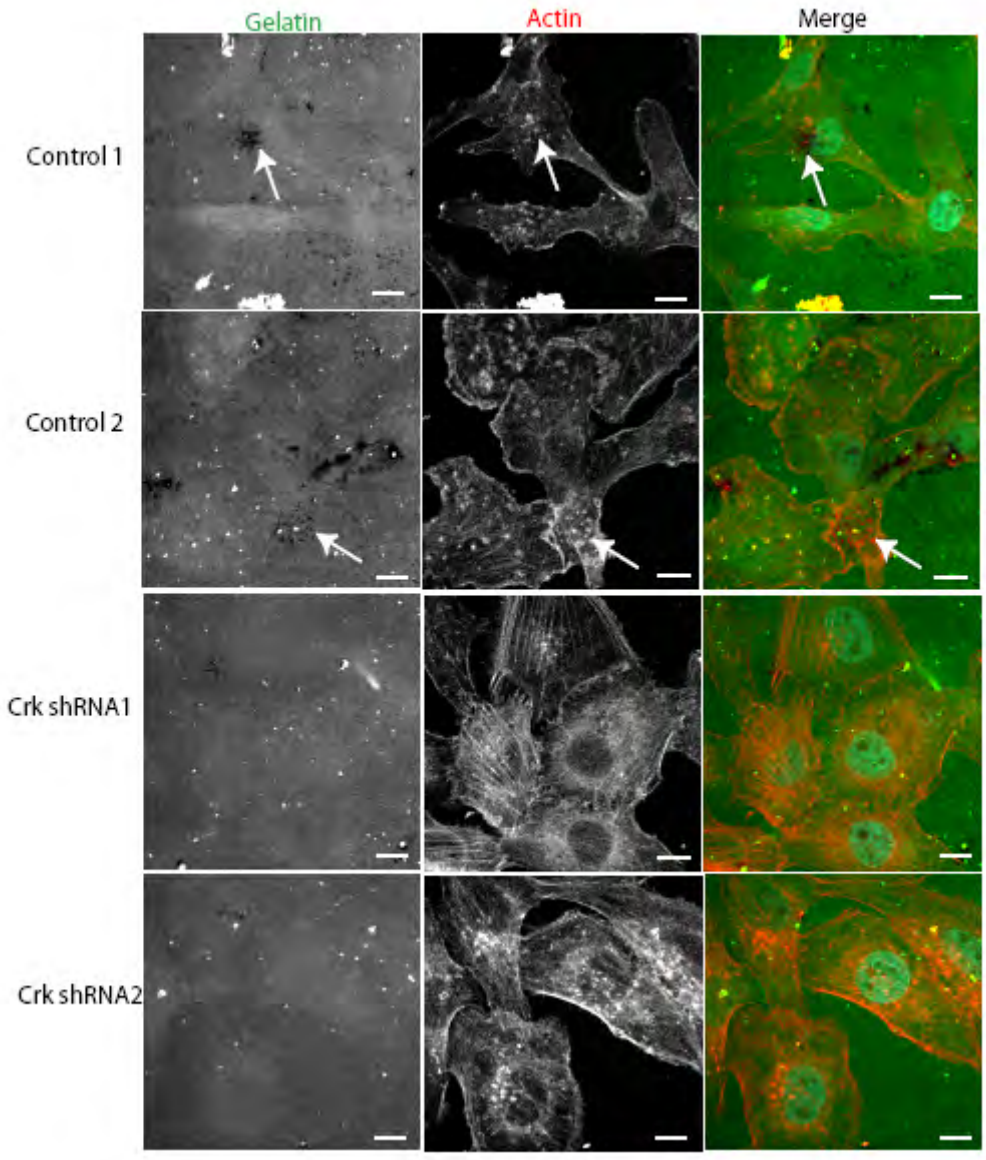

**Supplemental Figure 3 – Altered localization of phosphorylated Fak and p130Cas is observed in Crk shRNA cells, relative to control 1833TR cells.** Both control 1833TR and Crk shRNA cells were plated on collagen for 24 hours before fixation and staining for phosphorylated FAK and p130Cas. The localization of FAK and p130Cas is prominent at sites of membrane ruffling in control 1833TR cells, whereas in Crk shRNA cells, phosphorylated FAK and p130Cas is mainly in the cytosol.

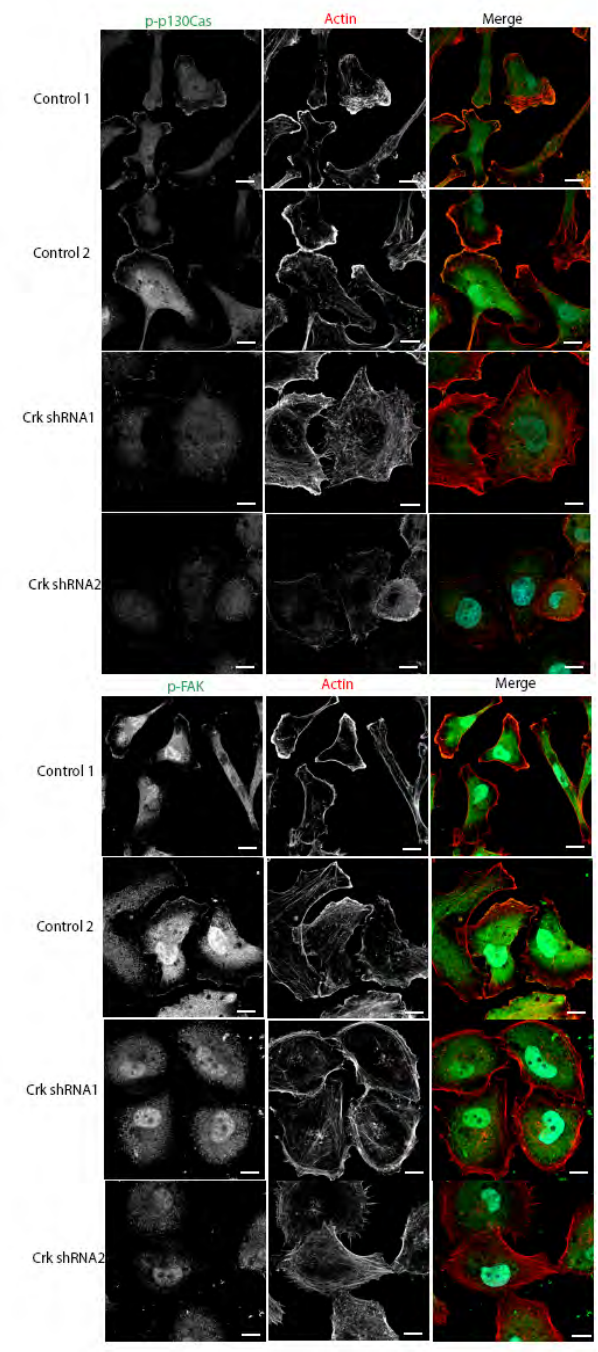

**Supplemental Figure 4 – Crk knockdown in MDA231TR parental cells results in changes in gene expression.** Western blot analysis of whole cell lysates (MDA-231TR) with an anti-CrkI/II or anti-CrkL sera revealed that the CrkI/II and CrkL siRNA transfected cells efficiently and specifically target their respective RNA. Actin protein levels were used as a loading control (A). Hierarchical clustering of all transfected samples reveal the scrambled siRNAs are more closely related to another than to the Crk knockdown samples and vice versa (B). Heatmap analysis demonstrates global changes in gene expression between the scrambled controls and the Crk knockdown samples (C).

**Supplemental Figure 4**

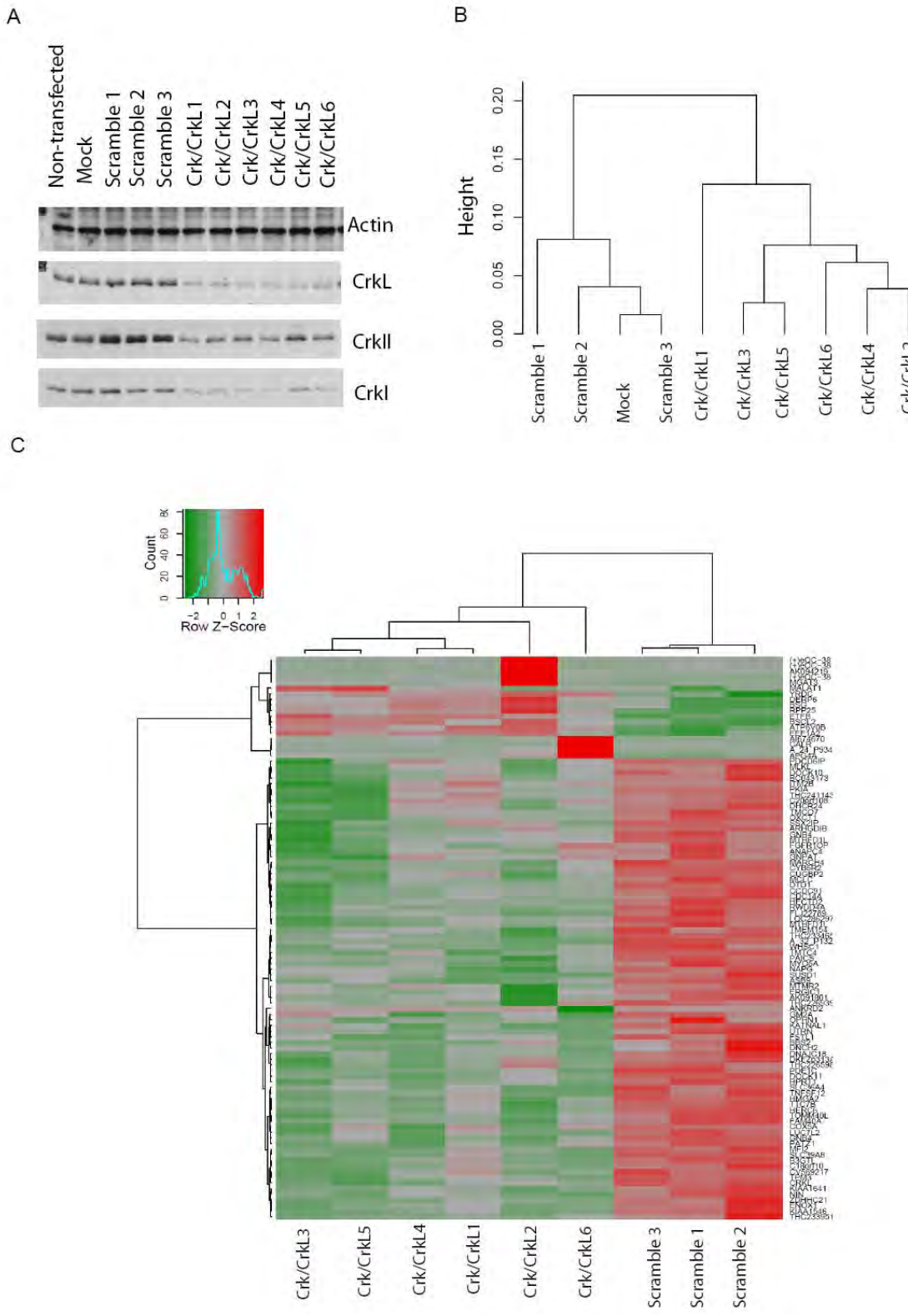


**Supplemental Figure 5 – Crk knockdown in MDA231TR parental cells results in changes**

**in gene expression of genes whose functions are important for tumour progression.** KEGG pathway analysis demonstrates several different pathways up-regulated or down-regulated in the Crk knockdown cells relative to the scrambled controls (A). Quantitative real-time PCR analysis identifies loss of Crk, CrkL and caveolin 2 in the Crk knockdown cells relative to the scrambled cells (B).

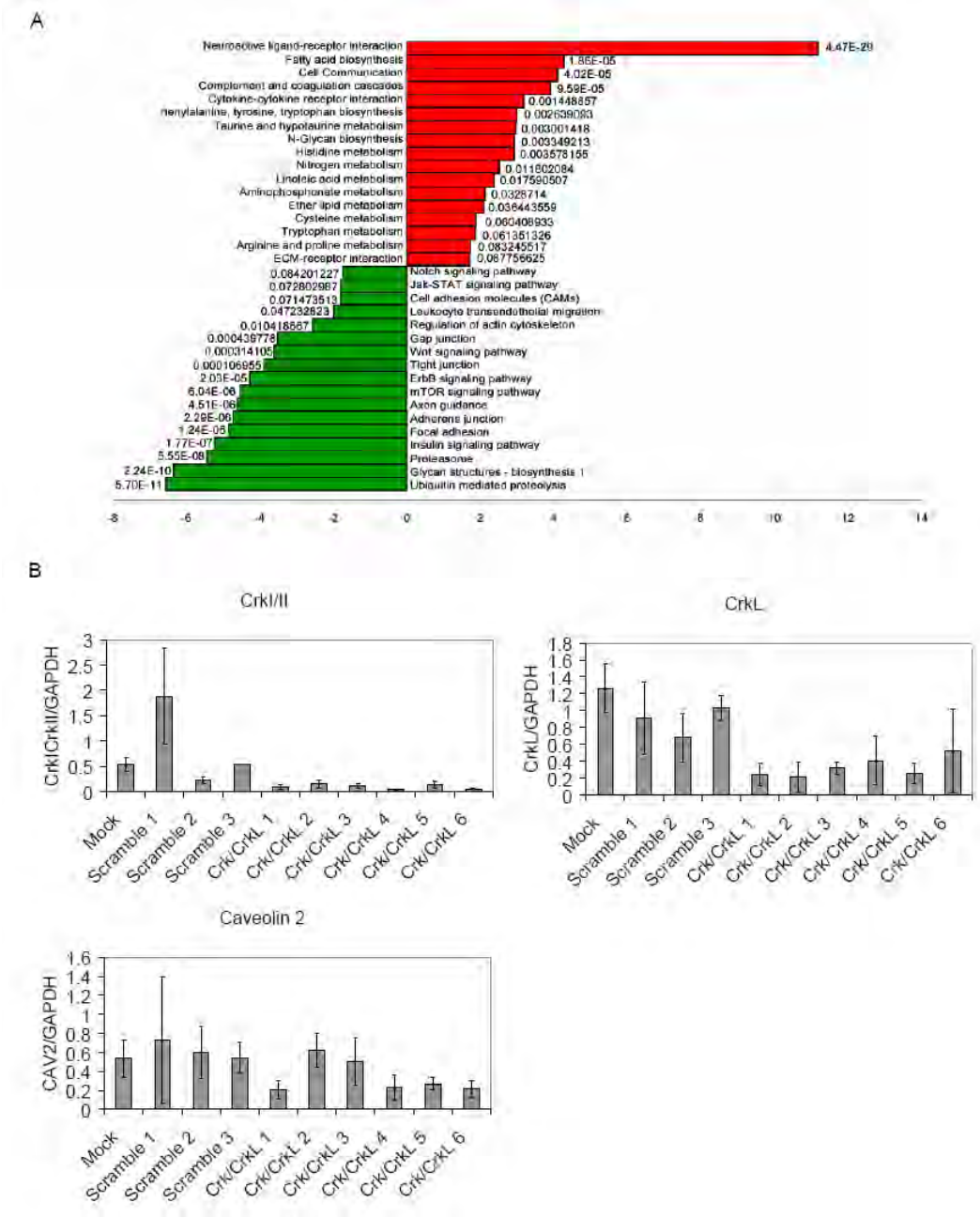


**Supplemental Figure 6 - GO pathway analysis.** Summary of GO biological processes (A) and

molecular functions (B) altered in the Crk knockdown cells relative to the controls.

A

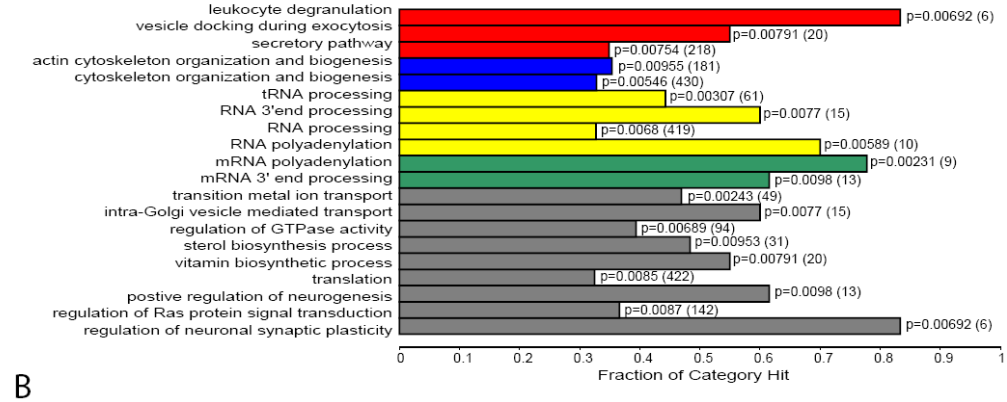


B

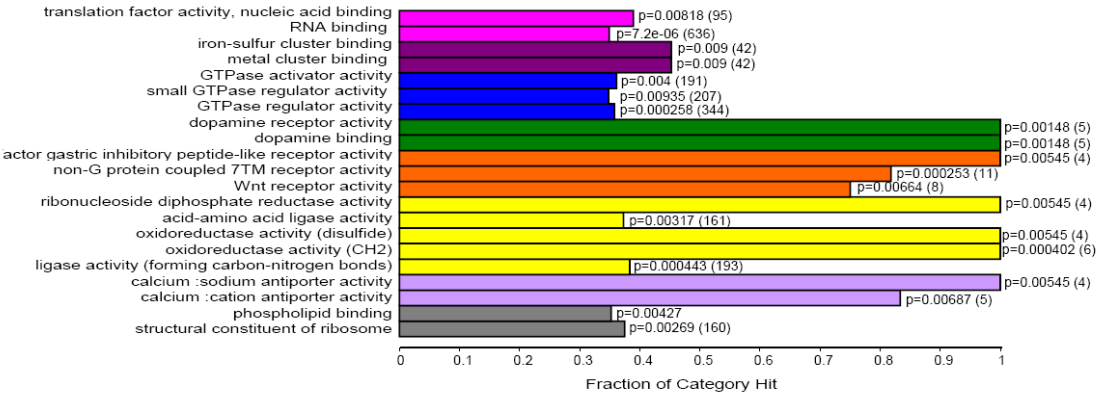


**Supplemental Table 2 - Common genes from the microarray data derived from the 1833TR**

**cell lines and the transient siRNA microarray data derived from the parental MDA-231 TR cell lines.** The fold change is the comparison between the Crk knockdown samples relative to the controls (ie. IL13RA2 is 13.7 fold lower in the Crk shRNA cells relative to the control cells.)

| Gene Name | 1833TR Fold Change | 1833TR p value | TR Fold Change | TR p value | Full gene name |
|---|---|---|---|---|---|
| IL13RA2 | -13.6808939 | 0.0002347 | -1.98646 | 0.01921 | interleukin 13 receptor, alpha 2 |
| VNN1 | -6.95535264 | 1.78E-05 | -1.63787 | 0.0068 | vanin 1 |
| LOC254848 | -6.13293017 | 7.25E-06 | -1.35131 | 0.03108 | hypothetical protein LOC254848 |
| FAM133A | -5.65761095 | 0.0055752 | -1.85332 | 0.0248 | family with sequence similarity 133, member A |
| TMEM46 | -4.78836403 | 0.0083533 | -1.63827 | 0.04869 | transmembrane protein 46 |
| BM921567 | -4.40264123 | 0.0038649 | -1.78387 | 0.01359 | NA |
| DGAT2 | -4.30853428 | 0.0159685 | -1.66367 | 0.04765 | diacylglycerol O-acyltransferase homolog 2 (mouse) |
| SAA4 | -4.22720126 | 0.0257297 | -1.6798 | 0.04394 | serum amyloid A4, constitutive |
| DGAT2 | -4.1959465 | 0.009523 | -1.69376 | 0.02921 | diacylglycerol O-acyltransferase homolog 2 (mouse) |
| LMO2 | -4.13032901 | 1.65E-05 | -1.56137 | 0.00273 | LIM domain only 2 (rhombotin-like 1) |
| FAM133A | -4.02132751 | 0.0085004 | -2.49403 | 0.00172 | family with sequence similarity 133, member A |
| A_24_P745883 | -4.00791219 | 1.79E-09 | -1.22379 | 0.00191 | NA |
| TNIP3 | -3.76144159 | 0.0182833 | -1.6925 | 0.03146 | TNFAIP3 interacting protein 3 |
| ADAMTS9 | -3.66556454 | 1.26E-05 | -1.49397 | 0.00202 | ADAM metallopeptidase with thrombospondin type 1 motif, 9 |
| DIAPH2 | -3.64715144 | 4.86E-05 | -1.58329 | 0.00201 | diaphanous homolog 2 (Drosophila) |
| ATP8A2 | -3.35423604 | 6.27E-08 | -1.23264 | 0.00402 | ATPase, aminophospholipid transporter-like, Class I, type 8A, member 2 |
| ABI3BP | -3.34420874 | 5.97E-06 | -1.27316 | 0.01327 | ABI gene family, member 3 (NESH) binding protein |
| BCL2A1 | -3.32913346 | 0.0245678 | -1.55912 | 0.04941 | BCL2-related protein A1 |
| RNF125 | -3.07302977 | 1.30E-08 | -1.1706 | 0.00609 | ring finger protein 125 |

| | | | | | |
|---|---|---|---|---|---|
| AKR1C1 | -2.91509637 | 0.0003373 | -1.31558 | 0.02483 | aldo-keto reductase family 1, member C1 (dihydrodiol dehydrogenase 1; 20-alpha (3-alpha)-hydroxysteroid dehydrogenase) |
| SLC16A2 | -2.89319015 | 0.0020676 | -1.67603 | 0.00336 | solute carrier family 16, member 2 (monocarboxylic acid transporter 8) |
| CD8A | -2.8900828 | 1.57E-05 | -1.20112 | 0.03501 | CD8a molecule |
| FAT3 | -2.80630465 | 3.19E-07 | -1.14631 | 0.02593 | FAT tumour suppressor homolog 3 (Drosophila) |
| GALNT14 | -2.78894489 | 0.0026633 | -1.4924 | 0.01104 | UDP-N-acetyl-alpha-D-galactosamine:polypeptide N-acetylgalactosaminyltransferase 14 (GalNAc-T14) |
| MIG7 | -2.78457371 | 0.0097971 | -1.78427 | 0.00429 | mig-7 |
| PAGE2 | -2.73056308 | 0.032266 | -1.67383 | 0.01602 | P antigen family, member 2 (prostate associated) |
| BX537688 | -2.65258648 | 0.0257571 | -2.06338 | 0.00209 | hypothetical LOC654433 |
| CORO2B | -2.61349029 | 9.61E-08 | -1.1058 | 0.04292 | coronin, actin binding protein, 2B |
| BIN1 | -2.5963029 | 0.0061543 | -1.46505 | 0.01595 | bridging integrator 1 |
| HRASLS | -2.50614313 | 0.0008531 | -1.47169 | 0.00419 | HRAS-like suppressor |
| RAGE | -2.50100421 | 5.84E-06 | -1.18823 | 0.01685 | renal tumour antigen |
| HLA-DPB1 | -2.49480976 | 0.016417 | -1.37659 | 0.04783 | major histocompatibility complex, class II, DP beta 1 |
| FHOD3 | -2.47463527 | 0.0335784 | -1.67929 | 0.01016 | formin homology 2 domain containing 3 |
| NSBP1 | -2.41706444 | 7.76E-05 | -1.37744 | 0.00899 | nucleosomal binding protein 1 |
| LAPTM5 | -2.41549233 | 0.0481303 | -1.45093 | 0.04642 | lysosomal associated multispanning membrane protein 5 |
| RBM41 | -2.40438669 | 3.29E-07 | -1.11133 | 0.03818 | RNA binding motif protein 41 |
| NEO1 | -2.36062657 | 0.0014895 | -1.35963 | 0.01199 | neogenin homolog 1 (chicken) |
| HLA-DMB | -2.33012835 | 0.0008432 | -1.2728 | 0.02423 | major histocompatibility complex, class II, DM beta |
| CABYR | -2.27244577 | 0.0404844 | -1.61087 | 0.01094 | calcium binding tyrosine-(Y)-phosphorylation regulated (fibrousheathin 2) |
| CTSW | -2.23358201 | 0.0495172 | -1.50863 | 0.02239 | cathepsin W |

| | | | | | |
|---|---|---|---|---|---|
| BC034319 | -2.14380172 | 0.0371169 | -1.48338 | 0.01704 | NA |
| SSPN | -2.12287155 | 0.0003169 | -1.31315 | 0.00517 | sarcospan (Kras oncogene-associated gene) |
| MCFD2 | -2.1194618 | 0.0340585 | -1.50201 | 0.01323 | multiple coagulation factor deficiency 2 |
| SLC26A7 | -2.1162635 | 0.0007071 | -1.29376 | 0.00995 | solute carrier family 26, member 7 |
| BE064950 | -2.11454639 | 9.38E-08 | -1.16256 | 0.00201 | NA |
| CRADD | -2.08512481 | 0.0039307 | -1.45898 | 0.00373 | CASP2 and RIPK1 domain containing adaptor with death domain |
| SEMA7A | -2.08122765 | 0.0001422 | -1.18935 | 0.02388 | semaphorin 7A, GPI membrane anchor (John Milton Hagen blood group) |
| BCL2A1 | -2.07305055 | 0.0035873 | -1.27631 | 0.02505 | BCL2-related protein A1 |
| ARHGAP30 | -2.05222232 | 0.0003482 | -1.21537 | 0.01989 | Rho GTPase activating protein 30 |
| APXL | -2.02576126 | 0.0072438 | -1.25537 | 0.04206 | shroom family member 2 |
| A_24_P24786 | -1.9856981 | 0.0425859 | -1.52914 | 0.00846 | NA |
| OR2A9P | -1.96786149 | 0.0131544 | -1.37095 | 0.01313 | olfactory receptor, family 2, subfamily A, member 9 pseudogene |
| AK023472 | -1.96523986 | 0.0017398 | -1.28065 | 0.01178 | NA |
| A_24_P341078 | -1.95929581 | 0.0409962 | -1.35986 | 0.03062 | NA |
| LIMD2 | -1.94477418 | 0.0129492 | -1.49951 | 0.00368 | LIM domain containing 2 |
| C1orf21 | -1.94339396 | 0.0243355 | -1.42508 | 0.01097 | chromosome 1 open reading frame 21 |
| DLG3 | -1.9379978 | 0.0196697 | -1.38303 | 0.01378 | discs, large homolog 3 (neuroendocrine-dlg, Drosophila) |
| SATB1 | -1.93641722 | 4.22E-05 | -1.17597 | 0.01194 | SATB homeobox 1 |
| MGC17624 | -1.93329959 | 5.25E-05 | -1.18872 | 0.00989 | chromosome 16 open reading frame 74 |
| ALDH2 | -1.93030659 | 0.0424135 | -1.52736 | 0.00698 | aldehyde dehydrogenase 2 family (mitochondrial) |
| ARHGEF4 | -1.92492665 | 0.005376 | -1.35665 | 0.00732 | Rho guanine nucleotide exchange factor (GEF) 4 |
| ENST00000331306 | -1.91166031 | 0.0156162 | -1.256 | 0.0455 | NA |
| AHNAK | -1.91105841 | 0.0033596 | -1.30005 | 0.01053 | AHNAK nucleoprotein |
| CSTF2 | -1.9105459 | 0.0005065 | -1.22561 | 0.01234 | cleavage stimulation factor, 3' pre-RNA, subunit 2, 64kDa |
| CYB5R2 | -1.90835 | 2.86E-05 | -1.32547 | 0.00039 | NA |
| PLXDC2 | -1.89938929 | 0.0176651 | -1.44437 | 0.00622 | plexin domain containing 2 |
| ENOX1 | -1.88587167 | 0.0166233 | -1.97803 | 0.00011 | ecto-NOX disulfide-thiol exchanger 1 |

| | | | | | |
|---|---|---|---|---|---|
| GBP5 | -1.85630895 | 0.0366746 | -1.48781 | 0.00631 | guanylate binding protein 5 |
| BHLHB9 | -1.85050455 | 0.0109531 | -1.43521 | 0.00388 | basic helix-loop-helix domain containing, class B, 9 |
| ENST00000338548 | -1.83627694 | 0.0002889 | -1.14424 | 0.04113 | NA |
| MCTS1 | -1.83589089 | 0.0349407 | -1.27297 | 0.04685 | malignant T cell amplified sequence 1 |
| MGC39900 | -1.83584725 | 0.0002486 | -1.16783 | 0.02199 | hypothetical protein MGC39900 |
| CXorf39 | -1.81869383 | 0.0322462 | -1.40517 | 0.01011 | chromosome X open reading frame 39 |
| KCNAB2 | -1.80434013 | 3.25E-05 | -1.13777 | 0.01763 | potassium voltage-gated channel, shaker-related subfamily, beta member 2 |
| OSBPL5 | -1.79831249 | 0.0112158 | -1.23266 | 0.03602 | oxysterol binding protein-like 5 |
| ARMCX1 | -1.79718876 | 0.0340051 | -1.27046 | 0.04181 | armadillo repeat containing, X-linked 1 |
| C4orf26 | -1.79068675 | 0.0045879 | -1.34706 | 0.00426 | chromosome 4 open reading frame 26 |
| PAK6 | -1.78572697 | 0.0041881 | -1.31004 | 0.00631 | p21(CDKN1A)-activated kinase 6 |
| Mar-01 | -1.78047918 | 0.0215903 | -1.34214 | 0.01215 | membrane-associated ring finger (C3HC4) 1 |
| Mar-01 | -1.75814375 | 0.0002526 | -1.21366 | 0.006 | membrane-associated ring finger (C3HC4) 1 |
| CASP1 | -1.756368 | 0.0065444 | -1.41851 | 0.00192 | caspase 1, apoptosis-related cysteine peptidase (interleukin 1, beta, convertase) |
| REPS2 | -1.74630806 | 0.0174255 | -1.30299 | 0.01462 | RALBP1 associated Eps domain containing 2 |
| ENST00000309379 | -1.73297253 | 0.0160837 | -1.2615 | 0.02259 | NA |
| RPL13 | -1.71966264 | 0.0036394 | -1.1648 | 0.04898 | ribosomal protein L13 |
| A_24_P349489 | -1.71662999 | 0.0057871 | -1.33491 | 0.004 | NA |
| BC031314 | -1.70815481 | 0.0003549 | -1.15433 | 0.02123 | NA |
| PIK3CD | -1.70365979 | 0.0471282 | -1.26888 | 0.03696 | phosphoinositide-3-kinase, catalytic, delta polypeptide |
| CTSS | -1.69905997 | 0.011178 | -1.26429 | 0.01475 | cathepsin S |
| BHLHB3 | -1.69671795 | 0.0265229 | -1.28629 | 0.01926 | basic helix-loop-helix domain containing, class B, 3 |
| DPF3 | -1.68457885 | 0.0015336 | -1.30568 | 0.00201 | D4, zinc and double PHD fingers, family 3 |
| THC2265983 | -1.66678939 | 0.0115145 | -1.81302 | 3.88E-05 | NA |
| A_24_P144383 | -1.64540667 | 0.0429059 | -1.38443 | 0.00657 | NA |
| THC2343435 | -1.64277481 | 0.0077242 | -1.23129 | 0.01496 | NA |

| | | | | | |
|---|---|---|---|---|---|
| BC071811 | -1.63352208 | 0.0468525 | -1.29528 | 0.01894 | similar to R28379_1 |
| A_32_P153361 | -1.62613524 | 0.0277247 | -1.30059 | 0.01133 | NA |
| THC2334681 | -1.62335138 | 0.0006568 | -1.20085 | 0.00619 | NA |
| IL13RA1 | -1.61817573 | 0.0234823 | -1.29791 | 0.0099 | interleukin 13 receptor, alpha 1 |
| LOC649839 | -1.60859252 | 0.0498451 | -1.24279 | 0.03543 | similar to large subunit ribosomal protein L36a |
| EMR1 | -1.59692192 | 0.0017219 | -1.15911 | 0.02238 | egf-like module containing, mucin-like, hormone receptor-like 1 |
| SLC25A5 | -1.58342009 | 0.0202321 | -1.20432 | 0.03115 | solute carrier family 25 (mitochondrial carrier; adenine nucleotide translocator), member 5 |
| ENST00000078131 | -1.58182253 | 0.0135808 | -1.17496 | 0.04223 | NA |
| A_24_P298228 | -1.5809011 | 6.92E-05 | -1.17477 | 0.00257 | NA |
| RPL30 | -1.58047881 | 0.0121669 | -1.21556 | 0.01829 | ribosomal protein L30 |
| DVL1 | -1.55435247 | 0.0386317 | -1.23429 | 0.0246 | dishevelled, dsh homolog 1 (Drosophila) |
| DDIT4L | -1.53187783 | 0.0005879 | -1.12246 | 0.02534 | DNA-damage-inducible transcript 4-like |
| PKIA | -1.5290402 | 0.0115972 | -1.49297 | 0.00021 | protein kinase (cAMP-dependent, catalytic) inhibitor alpha |
| ICAM2 | -1.52668924 | 0.0220377 | -1.18344 | 0.03503 | intercellular adhesion molecule 2 |
| LOC286044 | -1.52610283 | 0.0335411 | -1.19792 | 0.03494 | hypothetical protein LOC286044 |
| PDZK11 | -1.51044488 | 0.0211305 | -1.24692 | 0.0097 | PDZ domain containing 11 |
| APBB1 | -1.49900018 | 0.0001349 | -1.12767 | 0.00857 | amyloid beta (A4) precursor protein-binding, family B, member 1 (Fe65) |
| SLC25A5 | -1.49640387 | 0.0351928 | -1.2687 | 0.00904 | solute carrier family 25 (mitochondrial carrier; adenine nucleotide translocator), member 5 |
| CYP26B1 | -1.45880527 | 0.019056 | -1.20533 | 0.01287 | cytochrome P450, family 26, subfamily B, polypeptide 1 |
| MRPL30 | -1.45076981 | 0.0455216 | -1.1879 | 0.03143 | mitochondrial ribosomal protein L30 |
| ENST00000295249 | -1.44815529 | 0.0149138 | -1.16683 | 0.02271 | NA |
| DOCK11 | -1.44364184 | 0.0399542 | -1.63673 | 6.43E-05 | dedicator of cytokinesis 11 |
| A_32_P9924 | -1.43763982 | 0.0219257 | -1.25438 | 0.00478 | NA |
| PIK3CD | -1.43006431 | 0.0266865 | -1.2928 | 0.00262 | phosphoinositide-3-kinase, catalytic, delta polypeptide |

| | | | | | |
|---|---|---|---|---|---|
| FDFT1 | -1.41977931 | 0.0220704 | -1.29378 | 0.00199 | farnesyl-diphosphate farnesyltransferase 1 |
| F8 | -1.41313945 | 0.0030824 | -1.13668 | 0.01507 | coagulation factor VIII, procoagulant component (hemophilia A) |
| PMVK | -1.40771948 | 0.0466899 | -1.16201 | 0.03936 | phosphomevalonate kinase |
| A_24_P233560 | -1.3895796 | 0.0032768 | -1.11894 | 0.02192 | NA |
| MCC | -1.38745841 | 0.0073252 | -1.19397 | 0.0044 | mutated in colorectal cancers |
| THC2400010 | -1.37939888 | 0.0410653 | -1.19337 | 0.01422 | NA |
| A_24_P32930 | -1.37652361 | 0.0050943 | -1.14299 | 0.01166 | NA |
| ENST00000332097 | -1.37433853 | 0.0040694 | -1.13106 | 0.0145 | NA |
| TYW3 | -1.36917036 | 0.0073275 | -1.16343 | 0.00766 | tRNA-yW synthesizing protein 3 homolog (S. cerevisiae) |
| THAP3 | -1.35872666 | 0.0235096 | -1.12474 | 0.04205 | THAP domain containing, apoptosis associated protein 3 |
| POLK | -1.35817485 | 0.0233707 | -1.14594 | 0.02314 | polymerase (DNA directed) kappa |
| DNAJC7 | -1.32654408 | 0.0389278 | -1.24147 | 0.00262 | DnaJ (Hsp40) homolog, subfamily C, member 7 |
| PITPNC1 | -1.31351127 | 0.0168194 | -1.19915 | 0.00265 | phosphatidylinositol transfer protein, cytoplasmic 1 |
| ENST00000319163 | -1.30846371 | 0.0092078 | -1.13425 | 0.01007 | NA |
| A_24_P533142 | -1.30242141 | 0.0114302 | -1.21543 | 0.00107 | NA |
| SMAP-1 | -1.29243741 | 0.0191719 | -1.10985 | 0.02963 | unc-45 homolog A (C. elegans) |
| ADAMTSL1 | -1.28376428 | 0.0026453 | -1.07378 | 0.04068 | ADAMTS-like 1 |
| OPHN1 | -1.2780599 | 0.0080402 | -1.27105 | 0.00011 | oligophrenin 1 |
| A_24_P255836 | -1.27390676 | 0.0274754 | -1.10337 | 0.0371 | NA |
| C10orf118 | -1.26235548 | 0.0293211 | -1.12609 | 0.01545 | chromosome 10 open reading frame 118 |
| A_24_P928467 | -1.26108443 | 0.0471743 | -1.14314 | 0.01287 | NA |
| (+)E1A_r60_a97 | -1.25821705 | 0.0058342 | -1.09551 | 0.04635 | NA |
| (-)3xSLv1 | -1.18000607 | 0.0406061 | -1.29009 | 0.01646 | NA |
| SPRR2C | 1.219489706 | 0.0487437 | 1.086247 | 0.04897 | small proline-rich protein 2C |
| THC2318474 | 1.222897877 | 0.0493686 | 1.107441 | 0.02304 | NA |
| ZMAT2 | 1.226000727 | 0.0393321 | 1.093396 | 0.03503 | zinc finger, matrin type 2 |
| WDR40A | 1.235613892 | 0.0114054 | 1.110969 | 0.00879 | WD repeat domain 40A |
| PMS1 | 1.237871205 | 0.0099509 | 1.093621 | 0.01722 | PMS1 postmeiotic segregation increased 1 (S. cerevisiae) |
| ZMAT2 | 1.246395112 | 0.0234823 | 1.144395 | 0.00563 | zinc finger, matrin type 2 |
| THC2361927 | 1.263915582 | 0.0376765 | 1.141063 | 0.01178 | NA |

| | | | | | |
|---|---|---|---|---|---|
| KCNQ3 | 1.279251548 | 0.0325198 | 1.249684 | 0.00081 | potassium voltage-gated channel, KQT-like subfamily, member 3 |
| ZC3H13 | 1.280570554 | 0.0335266 | 1.144007 | 0.01271 | zinc finger CCCH-type containing 13 |
| THC2309461 | 1.293526414 | 0.0458248 | 1.115233 | 0.04428 | NA |
| GSTCD | 1.312390676 | 0.0484466 | 1.149364 | 0.02192 | glutathione S-transferase, C-terminal domain containing |
| ZXDC | 1.321275756 | 0.049164 | 1.137192 | 0.03376 | ZXD family zinc finger C |
| HERC4 | 1.325519563 | 0.0222685 | 1.134899 | 0.02172 | hect domain and RLD 4 |
| AF111705 | 1.331480211 | 0.0274521 | 1.13484 | 0.02662 | NA |
| THC2342574 | 1.338652977 | 0.0308973 | 1.127563 | 0.03814 | NA |
| NKTR | 1.339587076 | 0.0428055 | 1.177782 | 0.01363 | natural killer-tumour recognition sequence |
| THC2386560 | 1.345479717 | 0.0050399 | 1.090865 | 0.04934 | NA |
| SEMA4G | 1.352499411 | 0.033931 | 1.126055 | 0.04784 | sema domain, immunoglobulin domain (Ig), transmembrane domain (TM) and short cytoplasmic domain, (semaphorin) 4G |
| TIGD3 | 1.355746275 | 0.0094348 | 1.121904 | 0.02589 | tigger transposable element derived 3 |
| BX478538 | 1.356794685 | 0.0309512 | 1.126867 | 0.04603 | NA |
| AK026811 | 1.358912355 | 0.01575 | 1.151382 | 0.01564 | NA |
| A_24_P369172 | 1.366799981 | 0.0462777 | 1.146144 | 0.03991 | NA |
| PLEKHA4 | 1.376067722 | 0.0112942 | 1.173613 | 0.00839 | pleckstrin homology domain containing, family A (phosphoinositide binding specific) member 4 |
| GATA2 | 1.377594277 | 0.0102142 | 1.183247 | 0.00632 | GATA binding protein 2 |
| PRKY | 1.392638164 | 0.0057871 | 1.161639 | 0.00884 | protein kinase, Y-linked |
| Lin10 | 1.396976034 | 0.0340051 | 1.168896 | 0.0248 | chromosome 16 open reading frame 70 |
| IL17R | 1.398236048 | 0.0197677 | 1.158559 | 0.02203 | interleukin 17 receptor A |
| Lin10 | 1.398995844 | 0.0312931 | 1.168418 | 0.02399 | chromosome 16 open reading frame 70 |
| THC2364247 | 1.402130087 | 0.0042427 | 1.128762 | 0.02068 | NA |
| AK022252 | 1.402182188 | 0.0112942 | 1.120385 | 0.04503 | NA |
| B4GALT1 | 1.404297585 | 0.0335736 | 1.149205 | 0.04102 | UDP-Gal:betaGlcNAc beta 1,4-galactosyltransferase, polypeptide 1 |
| EP400 | 1.411526519 | 0.0061574 | 1.122992 | 0.03261 | E1A binding protein p400 |
| A_24_P885910 | 1.413251713 | 0.0066684 | 1.155221 | 0.01408 | NA |
| A_23_P320728 | 1.414359697 | 0.0219257 | 1.138862 | 0.04375 | NA |
| A_24_P936393 | 1.41917375 | 0.035701 | 1.21983 | 0.01102 | NA |

| | | | | | |
|---|---|---|---|---|---|
| TM7SF2 | 1.423834506 | 0.0037721 | 1.129243 | 0.02276 | transmembrane 7 superfamily member 2 |
| FTO | 1.428792063 | 0.0133908 | 1.133118 | 0.04257 | fat mass and obesity associated |
| LOC400987 | 1.431640246 | 0.0287546 | 1.198525 | 0.01584 | similar to ankyrin repeat domain 36 |
| TNRC6A | 1.434344329 | 0.0268836 | 1.183427 | 0.02113 | trinucleotide repeat containing 6A |
| TGFBRAP1 | 1.436105739 | 0.0024666 | 1.10281 | 0.04778 | transforming growth factor, beta receptor associated protein 1 |
| SNX3 | 1.438187731 | 0.0042312 | 1.132019 | 0.02526 | NA |
| ELL3 | 1.442620535 | 0.0209259 | 1.144277 | 0.04566 | elongation factor RNA polymerase II-like 3 |
| REPIN1 | 1.445029763 | 0.0115972 | 1.196375 | 0.00985 | replication initiator 1 |
| AF483645 | 1.448911276 | 0.0115544 | 1.166189 | 0.01995 | NA |
| CAMK2D | 1.466360314 | 0.0025657 | 1.16141 | 0.01077 | calcium/calmodulin-dependent protein kinase (CaM kinase) II delta |
| KIAA1666 | 1.479486005 | 0.0065444 | 1.160845 | 0.02058 | KIAA1666 protein |
| LSM14B | 1.480842423 | 0.0177632 | 1.157328 | 0.03982 | LSM14B, SCD6 homolog B (S. cerevisiae) |
| AF009267 | 1.483479042 | 0.0003361 | 1.118458 | 0.01609 | NA |
| ATP8B2 | 1.490301354 | 0.0148723 | 1.159069 | 0.03671 | ATPase, Class I, type 8B, member 2 |
| MGC22265 | 1.499412572 | 0.011371 | 1.256494 | 0.00482 | similar to Beta-glucuronidase precursor |
| NFATC3 | 1.49963418 | 0.0091896 | 1.308531 | 0.00172 | nuclear factor of activated T-cells, cytoplasmic, calcineurin-dependent 3 |
| THC2310998 | 1.526697637 | 0.0005706 | 1.113093 | 0.03261 | NA |
| AK095300 | 1.536588057 | 0.0002436 | 1.099395 | 0.03902 | NA |
| HDAC4 | 1.539648506 | 0.0001252 | 1.102479 | 0.02719 | histone deacetylase 4 |
| KRT86 | 1.544341163 | 0.0008404 | 1.127539 | 0.0276 | keratin 86 |
| C5orf32 | 1.54954483 | 0.0121804 | 1.208345 | 0.01722 | chromosome 5 open reading frame 32 |
| ZNF808 | 1.552180992 | 0.042414 | 1.223658 | 0.03093 | zinc finger protein 808 |
| ZNF700 | 1.563268406 | 0.0082012 | 1.206755 | 0.01523 | zinc finger protein 700 |
| BC042520 | 1.564094686 | 0.0051239 | 1.168521 | 0.02573 | NA |
| PCLO | 1.566486976 | 0.0217355 | 1.2039 | 0.02992 | piccolo (presynaptic cytomatrix protein) |
| GPRC5B | 1.571682087 | 0.0008431 | 1.216915 | 0.00358 | G protein-coupled receptor, family C, group 5, member B |
| C14orf113 | 1.580195458 | 4.30E-05 | 1.108672 | 0.01745 | chromosome 14 open reading frame 113 |
| MBNL1 | 1.58315443 | 0.0291186 | 1.194668 | 0.04623 | muscleblind-like (Drosophila) |
| MYO1B | 1.585567569 | 0.0093922 | 1.173294 | 0.03639 | myosin IB |

| | | | | | |
|---|---|---|---|---|---|
| DAF | 1.599681812 | 0.0175588 | 1.197804 | 0.03502 | CD55 molecule, decay accelerating factor for complement (Cromer blood group) |
| ELAVL4 | 1.617268115 | 0.0051611 | 1.159669 | 0.04173 | ELAV (embryonic lethal, abnormal vision, Drosophila)-like 4 (Hu antigen D) |
| PDPR | 1.631266685 | 0.0057166 | 1.276974 | 0.00561 | pyruvate dehydrogenase phosphatase regulatory subunit |
| NARG1 | 1.641568196 | 0.0019952 | 1.172107 | 0.02246 | NMDA receptor regulated 1 |
| KRT14 | 1.673710756 | 0.0110764 | 1.212565 | 0.02957 | keratin 14 (epidermolysis bullosa simplex, Dowling-Meara, Koebner) |
| TITF1 | 1.675090723 | 0.0057166 | 1.170094 | 0.0459 | NK2 homeobox 1 |
| MALAT1 | 1.682138387 | 0.0150424 | 1.752568 | 0.00011 | metastasis associated lung adenocarcinoma transcript 1 (non-coding RNA) |
| ZNF398 | 1.685333585 | 0.0044106 | 1.220895 | 0.01596 | zinc finger protein 398 |
| FLJ12331 | 1.688133188 | 0.000933 | 1.174067 | 0.01884 | ribosomal protein S2 pseudogene |
| VAC14 | 1.701789971 | 0.0001128 | 1.11784 | 0.03546 | Vac14 homolog (S. cerevisiae) |
| ZNF275 | 1.725122885 | 0.0005797 | 1.198125 | 0.01048 | zinc finger protein 275 |
| THC2304438 | 1.738456688 | 0.000431 | 1.206513 | 0.008 | NA |
| PLCB1 | 1.748595091 | 0.0002075 | 1.196321 | 0.00728 | phospholipase C, beta 1 (phosphoinositide-specific) |
| RDX | 1.753628709 | 0.0074925 | 1.196797 | 0.0439 | Radixin |
| MBOAT2 | 1.766398682 | 0.0012781 | 1.153815 | 0.04719 | membrane bound O-acyltransferase domain containing 2 |
| AP1G1 | 1.773995172 | 0.0006447 | 1.143065 | 0.04687 | adaptor-related protein complex 1, gamma 1 subunit |
| THC2281660 | 1.783818476 | 5.85E-06 | 1.106532 | 0.02288 | NA |
| SP100 | 1.794795216 | 0.0006117 | 1.178668 | 0.02211 | SP100 nuclear antigen |
| AK025323 | 1.803520438 | 0.0017967 | 1.211531 | 0.02011 | NA |
| MGC12982 | 1.811383568 | 0.0326676 | 1.280607 | 0.03786 | hypothetical protein MGC12982 |
| THC2376828 | 1.820496184 | 4.12E-05 | 1.129697 | 0.02621 | NA |
| BX108121 | 1.835692673 | 0.028526 | 1.267084 | 0.04453 | NA |
| ZNF66 | 1.854446016 | 0.00621 | 1.289894 | 0.01419 | zinc finger protein 66 |
| THC2378865 | 1.874059961 | 3.87E-05 | 1.139857 | 0.02305 | NA |
| ZNF708 | 1.939440159 | 0.0084596 | 1.267963 | 0.03024 | zinc finger protein 708 |

| | | | | | |
|---|---|---|---|---|---|
| HOM-TES-103 | 1.940294124 | 0.009876 | 1.35502 | 0.01164 | hypothetical protein LOC25900 |
| CCRK | 1.945342967 | 0.003511 | 1.283548 | 0.01527 | cell cycle related kinase |
| AF086536 | 1.962903505 | 0.008618 | 1.238184 | 0.04862 | NA |
| AK094623 | 1.963538562 | 8.98E-05 | 1.195756 | 0.01198 | NA |
| ZNF117 | 1.970594804 | 0.0051779 | 1.310292 | 0.01471 | zinc finger protein 117 |
| MOCOS | 1.972006941 | 0.0020982 | 1.188489 | 0.0459 | molybdenum cofactor sulfurase |
| IFIT2 | 1.985845558 | 0.0174709 | 1.290949 | 0.03939 | interferon-induced protein with tetratricopeptide repeats 2 |
| C5orf25 | 2.03473902 | 0.0006908 | 1.200851 | 0.03337 | chromosome 5 open reading frame 25 |
| THC2290974 | 2.040564558 | 0.028923 | 1.382786 | 0.02482 | NA |
| AA359500 | 2.054466601 | 0.0006861 | 1.267755 | 0.01178 | similar to nuclear pore membrane protein 121 |
| NANOS1 | 2.104863635 | 0.0002487 | 1.372429 | 0.00186 | nanos homolog 1 (Drosophila) |
| ZNF331 | 2.109759529 | 0.0011548 | 1.214267 | 0.04001 | zinc finger protein 331 |
| A_32_P205792 | 2.13152956 | 0.0051591 | 1.267883 | 0.03905 | NA |
| ZNF492 | 2.134487428 | 0.0009421 | 1.233215 | 0.02896 | zinc finger protein 492 |
| MLL | 2.142005066 | 1.92E-06 | 1.130949 | 0.02177 | myeloid/lymphoid or mixed-lineage leukemia (trithorax homolog, Drosophila) |
| ZNF100 | 2.165516612 | 0.0019355 | 1.269231 | 0.0258 | zinc finger protein 100 |
| THC2438118 | 2.172248115 | 0.0115544 | 1.34209 | 0.02878 | NA |
| APC2 | 2.181823113 | 6.91E-05 | 1.211391 | 0.01493 | adenomatosis polyposis coli 2 |
| FBXL7 | 2.182990385 | 3.29E-05 | 1.204467 | 0.01216 | F-box and leucine-rich repeat protein 7 |
| CH25H | 2.196168413 | 0.0001349 | 1.280209 | 0.00657 | cholesterol 25-hydroxylase |
| ZNF539 | 2.225650467 | 0.0042638 | 1.295457 | 0.03133 | zinc finger protein 254 |
| PRSS7 | 2.233104326 | 0.0239284 | 1.353533 | 0.04528 | protease, serine, 7 (enterokinase) |
| HIST1H2AC | 2.247090772 | 1.78E-06 | 1.128667 | 0.02865 | histone cluster 1, H2ac |
| ZNF430 | 2.248476407 | 0.0018432 | 1.235121 | 0.04832 | zinc finger protein 430 |
| THC2319755 | 2.282384896 | 0.0006908 | 1.218382 | 0.04421 | NA |
| FN1 | 2.390944617 | 0.0338647 | 1.542253 | 0.01904 | fibronectin 1 |
| ZNF682 | 2.395440728 | 0.0052608 | 1.372545 | 0.02219 | zinc finger protein 682 |
| ZNF708 | 2.398776945 | 0.0140002 | 1.397422 | 0.03113 | zinc finger protein 708 |
| THC2381319 | 2.701962825 | 4.59E-06 | 1.15481 | 0.04423 | NA |
| DKFZp779O175 | 2.768368159 | 0.008618 | 1.489181 | 0.0214 | hypothetical protein DKFZp779O175 |
| SHOX | 2.907257973 | 0.0002012 | 1.285548 | 0.02816 | short stature homeobox |
| THC2290002 | 3.169503218 | 0.0010781 | 1.329106 | 0.04714 | NA |
| PDE9A | 3.648639728 | 0.0111694 | 1.804233 | 0.01291 | phosphodiesterase 9A |

**Supplemental Table 3 -** Full list of KEGG pathway analysis results from stable MDA-231 1833TR microarray experiment.

| z | Pvalue | Description |
|---|---|---|
| -3.96361 | 7.38E-05 | Proteasome |
| -0.58248 | 0.560246 | Focal adhesion |
| -1.87466 | 0.060839 | Dorso-ventral axis formation |
| -0.89398 | 0.371334 | ECM-receptor interaction |
| -2.46339 | 0.013763 | SNARE interactions in vesicular transport |
| -1.65327 | 0.098275 | T cell receptor signaling pathway |
| -5.54983 | 2.86E-08 | Cell adhesion molecules (CAMs) |
| 2.742175 | 0.006103 | Biosynthesis of steroids |
| 0.663711 | 0.506875 | B cell receptor signaling pathway |
| 1.123703 | 0.261139 | Glyoxylate and dicarboxylate metabolism |
| -0.48893 | 0.624889 | Colorectal cancer |
| -2.58352 | 0.00978 | Aminophosphonate metabolism |
| -3.08488 | 0.002036 | Fc epsilon RI signaling pathway |
| -2.56157 | 0.01042 | Benzoate degradation via CoA ligation |
| -1.3157 | 0.188276 | Aminoacyl-tRNA biosynthesis |
| -2.59418 | 0.009482 | Renal cell carcinoma |
| -0.84958 | 0.395561 | Pancreatic cancer |
| -3.08386 | 0.002043 | Parkinson's disease |
| 1.083106 | 0.278761 | Endometrial cancer |
| -0.84826 | 0.396292 | Glutamate metabolism |
| 0.545702 | 0.585271 | Glioma |
| -1.22965 | 0.218828 | Alanine and aspartate metabolism |
| -4.97149 | 6.64E-07 | Arachidonic acid metabolism |
| -2.03197 | 0.042157 | Prostate cancer |
| -1.07858 | 0.280775 | Fatty acid biosynthesis |
| -4.49087 | 7.09E-06 | Linoleic acid metabolism |
| -0.85436 | 0.392904 | Thyroid cancer |
| -1.01346 | 0.31084 | Circadian rhythm |
| -2.44172 | 0.014617 | Fatty acid elongation in mitochondria |
| 0.123149 | 0.901989 | Basal cell carcinoma |
| 0.749357 | 0.453642 | Melanoma |
| -0.03814 | 0.969577 | Protein export |
| -0.52534 | 0.599348 | Adherens junction |
| -0.5471 | 0.584307 | Bladder cancer |
| -0.90197 | 0.367073 | Notch signaling pathway |
| -1.22063 | 0.222226 | Leukocyte transendothelial migration |
| -1.65482 | 0.09796 | Regulation of autophagy |
| -1.50514 | 0.132287 | Propanoate metabolism |

| | | |
|---|---|---|
| -2.5434 | 0.010978 | Chronic myeloid leukemia |
| -2.29952 | 0.021476 | Selenoamino acid metabolism |
| -0.53142 | 0.595129 | Ethylbenzene degradation |
| -5.25917 | 1.45E-07 | Metabolism of xenobiotics by cytochrome P450 |
| -1.54474 | 0.122408 | Acute myeloid leukemia |
| -0.33267 | 0.739383 | Small cell lung cancer |
| -1.22109 | 0.222053 | Amyotrophic lateral sclerosis (ALS) |
| -0.43687 | 0.662203 | Folate biosynthesis |
| -3.84639 | 0.00012 | Glycine, serine and threonine metabolism |
| 0.20136 | 0.840417 | Non-small cell lung cancer |
| -2.46348 | 0.013759 | Atrazine degradation |
| -1.96903 | 0.04895 | Insulin signaling pathway |
| -3.06174 | 0.002201 | Fatty acid metabolism |
| 0.317991 | 0.750492 | Long-term potentiation |
| 0.260549 | 0.79444 | Synthesis and degradation of ketone bodies |
| -0.75069 | 0.452837 | GnRH signaling pathway |
| -0.19253 | 0.84733 | Tight junction |
| 1.182804 | 0.236887 | Hedgehog signaling pathway |
| 0.913901 | 0.360769 | Melanogenesis |
| -0.84633 | 0.397366 | Starch and sucrose metabolism |
| -3.1167 | 0.001829 | Lysine degradation |
| -1.45212 | 0.146467 | mTOR signaling pathway |
| -2.16528 | 0.030367 | Bile acid biosynthesis |
| -2.2957 | 0.021693 | Butanoate metabolism |
| -0.63472 | 0.525612 | Cyanoamino acid metabolism |
| -2.71907 | 0.006547 | Huntington's disease |
| -0.00461 | 0.996322 | Methionine metabolism |
| -2.66502 | 0.007698 | Adipocytokine signaling pathway |
| -0.65473 | 0.512643 | Cysteine metabolism |
| -1.57877 | 0.11439 | Long-term depression |
| -2.3118 | 0.020789 | MAPK signaling pathway |
| 0.97068 | 0.331707 | Gap junction |
| -1.43153 | 0.152279 | ErbB signaling pathway |
| 0.116053 | 0.90761 | TGF-beta signaling pathway |
| -0.75321 | 0.451326 | N-Glycan biosynthesis |
| -0.21041 | 0.83335 | N-Glycan degradation |
| 1.096202 | 0.27299 | O-Glycan biosynthesis |
| -2.36798 | 0.017886 | Ubiquinone biosynthesis |
| -3.61939 | 0.000295 | PPAR signaling pathway |
| 0.533276 | 0.593843 | Dentatorubropallidoluysian atrophy (DRPLA) |
| -2.98285 | 0.002856 | Valine, leucine and isoleucine degradation |

| | | |
|---|---|---|
| -0.19095 | 0.848562 | Type II diabetes mellitus |
| -4.42305 | 9.73E-06 | Apoptosis |
| -0.7706 | 0.440943 | Terpenoid biosynthesis |
| -0.13431 | 0.89316 | Olfactory transduction |
| 0.267204 | 0.789312 | Calcium signaling pathway |
| -1.1777 | 0.238917 | Carbon fixation |
| 1.786254 | 0.074058 | Taste transduction |
| -3.22723 | 0.00125 | Limonene and pinene degradation |
| 0.820147 | 0.412132 | Axon guidance |
| -0.80897 | 0.418533 | Nucleotide sugars metabolism |
| -2.01237 | 0.044181 | Streptomycin biosynthesis |
| -3.7063 | 0.00021 | Arginine and proline metabolism |
| -2.10479 | 0.035309 | Porphyrin and chlorophyll metabolism |
| -1.08438 | 0.278198 | One carbon pool by folate |
| -0.91249 | 0.36151 | C21-Steroid hormone metabolism |
| -3.88556 | 0.000102 | Glutathione metabolism |
| 1.030907 | 0.302584 | Prion disease |
| 0.000381 | 0.999696 | Valine, leucine and isoleucine biosynthesis |
| -4.46397 | 8.05E-06 | Type I diabetes mellitus |
| -1.15754 | 0.247052 | Glycan structures - biosynthesis 1 |
| 0.294995 | 0.767998 | Glycan structures - biosynthesis 2 |
| -0.26994 | 0.787207 | Glycan structures – degradation |
| -4.03666 | 5.42E-05 | Nitrogen metabolism |
| 0.288851 | 0.772695 | Reductive carboxylate cycle (CO2 fixation) |
| -1.24292 | 0.213897 | Aminosugars metabolism |
| -0.28086 | 0.778817 | VEGF signaling pathway |
| -0.62584 | 0.531422 | Glycosaminoglycan degradation |
| -1.11754 | 0.263762 | Cholera – Infection |
| -3.29953 | 0.000968 | Histidine metabolism |
| -1.36388 | 0.172605 | Chondroitin sulfate biosynthesis |
| -1.93953 | 0.052437 | Keratan sulfate biosynthesis |
| -0.04901 | 0.960909 | Methane metabolism |
| -0.53952 | 0.589527 | Heparan sulfate biosynthesis |
| -2.9081 | 0.003636 | Androgen and estrogen metabolism |
| -1.93864 | 0.052545 | Complement and coagulation cascades |
| -1.75724 | 0.078877 | Maturity onset diabetes of the young |
| -4.75687 | 1.97E-06 | Antigen processing and presentation |
| 1.110029 | 0.266986 | Renin-angiotensin system |
| -0.1878 | 0.851036 | Sulfur metabolism |
| -1.2424 | 0.214087 | Thiamine metabolism |
| -3.0097 | 0.002615 | Glycolysis / Gluconeogenesis |

| | | |
|---|---|---|
| -2.49072 | 0.012748 | Epithelial cell signaling in Helicobacter pylori infection |
| -3.13259 | 0.001733 | Tyrosine metabolism |
| -4.56084 | 5.10E-06 | Ribosome |
| 0.266872 | 0.789568 | Regulation of actin cytoskeleton |
| 0.516822 | 0.60528 | Cell Communication |
| -4.98281 | 6.27E-07 | Toll-like receptor signaling pathway |
| -3.51463 | 0.00044 | Caprolactam degradation |
| -0.99768 | 0.318433 | Phenylalanine, tyrosine and tryptophan biosynthesis |
| -2.07878 | 0.037638 | Riboflavin metabolism |
| -3.26587 | 0.001091 | Citrate cycle (TCA cycle) |
| -2.08135 | 0.037401 | Pathogenic Escherichia coli infection – EHEC |
| -1.38214 | 0.166928 | Phenylalanine metabolism |
| -2.08135 | 0.037401 | Pathogenic Escherichia coli infection – EPEC |
| -0.48134 | 0.630271 | gamma-Hexachlorocyclohexane degradation |
| -1.93953 | 0.052436 | RNA polymerase |
| 0.388889 | 0.697358 | Benzoate degradation via hydroxylation |
| -1.06429 | 0.287198 | Bisphenol A degradation |
| -1.1039 | 0.269635 | Basal transcription factors |
| -2.03174 | 0.04218 | Jak-STAT signaling pathway |
| -2.04295 | 0.041057 | Sphingolipid metabolism |
| -0.37537 | 0.707384 | Glycosphingolipid biosynthesis – lactoseries |
| 0.177007 | 0.859503 | Glycosphingolipid biosynthesis - neo-lactoseries |
| -0.40727 | 0.68381 | Phenylpropanoid biosynthesis |
| -1.74998 | 0.080121 | beta-Alanine metabolism |
| -1.72628 | 0.084297 | Glycosphingolipid biosynthesis – globoseries |
| -2.22135 | 0.026327 | Glycosphingolipid biosynthesis – ganglioseries |
| -3.52427 | 0.000425 | Urea cycle and metabolism of amino groups |
| -4.41297 | 1.02E-05 | Cytokine-cytokine receptor interaction |
| -2.55843 | 0.010515 | Vitamin B6 metabolism |
| -4.54259 | 5.56E-06 | Pentose phosphate pathway |
| -3.17318 | 0.001508 | Glycerolipid metabolism |
| 1.016877 | 0.309212 | Inositol phosphate metabolism |
| 1.970217 | 0.048813 | Glycosylphosphatidylinositol(GPI)-anchor biosynthesis |
| -2.32375 | 0.020139 | Glycerophospholipid metabolism |
| -0.59303 | 0.553164 | DNA polymerase |
| -2.42503 | 0.015307 | Ether lipid metabolism |
| 0.573646 | 0.566207 | Cell cycle |
| -3.29181 | 0.000995 | Hematopoietic cell lineage |
| -0.11686 | 0.906969 | Alkaloid biosynthesis I |
| -0.71305 | 0.475816 | p53 signaling pathway |
| -4.31468 | 1.60E-05 | Purine metabolism |

| | | |
|---|---|---|
| 0.424351 | 0.67131 | Phosphatidylinositol signaling system |
| -5.59757 | 2.17E-08 | Nicotinate and nicotinamide metabolism |
| -0.95021 | 0.342005 | Pentose and glucuronate interconversions |
| -3.08843 | 0.002012 | Tryptophan metabolism |
| -5.54344 | 2.97E-08 | Oxidative phosphorylation |
| 2.454983 | 0.014089 | Wnt signaling pathway |
| 1.540028 | 0.123554 | Ubiquitin mediated proteolysis |
| -1.90172 | 0.057208 | Natural killer cell mediated cytotoxicity |
| 0.619866 | 0.535346 | ABC transporters – General |
| -2.02786 | 0.042574 | Pyruvate metabolism |
| -1.2663 | 0.205404 | Taurine and hypotaurine metabolism |
| 0.985638 | 0.324311 | Alkaloid biosynthesis II |
| 1.434173 | 0.151523 | 2,4-Dichlorobenzoate degradation |
| -3.19351 | 0.001406 | Alzheimer's disease |
| -1.18045 | 0.237823 | Neuroactive ligand-receptor interaction |
| -2.67561 | 0.007459 | Pantothenate and CoA biosynthesis |
| -0.49189 | 0.622795 | 1- and 2-Methylnaphthalene degradation |
| -3.68216 | 0.000231 | Pyrimidine metabolism |
| -1.65858 | 0.097201 | Tetrachloroethene degradation |
| -1.77187 | 0.076416 | Neurodegenerative Disorders |
| -2.79865 | 0.005132 | Naphthalene and anthracene degradation |
| -2.68845 | 0.007178 | Fructose and mannose metabolism |
| -3.27395 | 0.001061 | Galactose metabolism |
| -2.43123 | 0.015048 | Ascorbate and aldarate metabolism |

**Supplemental Table 4** - Full list of GO terms (Biological Processes and Molecular Functions) from stable MDA-231 1833TR knockdown, where t equals the total number of genes in that particular category, r represents the number of genes affected in the Control versus Crk knockdown comparision and p represents the statistically significant p-value.

| Biological Processes | T | R | P |
|---|---|---|---|
| Regulation of global transcription from RNA polymerase II promoter | 4 | 3 | 0.00224 |
| Regulation of transcription, DNA dependent | 2016 | 216 | 5.23E-05 |
| Transcription, DNA dependent | 2070 | 219 | 0.000102 |
| Regulation of transcription | 2141 | 227 | 6.33E-05 |
| RNA biosynthetic process | 2074 | 230 | 8.27E-05 |
| Transcription | 2231 | 230 | 0.000326 |
| RNA metabolic process | 2546 | 251 | 2.36E-03 |
| Sterol biosynthetic process | 31 | 8 | 3.38E-03 |
| DNA packaging | 286 | 48 | 2.81E-06 |
| DNA metabolic process | 675 | 76 | 5.25E-03 |
| Nucleosome assembly | 76 | 27 | 3.61E-11 |
| Protein-DNA complex assembly | 135 | 37 | 6.18E-11 |
| Chromatin assembly | 87 | 29 | 4.12E-11 |
| Establishment and/or maintenance of chromatin structure | 280 | 48 | 1.52E-06 |
| Regulation of nucleobase, nucleoside, nucleotide, and nucleic acid metabolic process | 2199 | 229 | 1.83E-04 |
| Nucleobase, nucleoside, nucleotide, and nucleic acid metabolic process | 3327 | 332 | 1.25E-04 |
| NAD biosynthetic process | 6 | 3 | 9.83E-03 |
| NAD metabolic process | 6 | 3 | 9.83E-03 |
| Cellular component pathway | 531 | 68 | 3.03E-04 |
| Chromosome organization and biogenesis | 346 | 52 | 2.80E-05 |
| Golgi organization and biogenesis | 10 | 4 | 0.00696 |
| Organelle organization and biogenesis | 998 | 115 | 1.77E-04 |
| Cellular component organization and biogenesis | 2315 | 225 | 8.15E-03 |
| Cytoskeletal anchoring | 10 | 4 | 0.00696 |
| Regulation of cellular metabolic process | 2375 | 246 | 1.38E-04 |
| Extracellular structure organization and biogenesis | 72 | 14 | 2.43E-03 |
| Regulation of metabolic process | 2462 | 250 | 4.34E-04 |
| Negative regulation of smooth muscle cell differentiation | 2 | 2 | 7.01E-03 |

| | | | |
|---|---|---|---|
| Regulation of smooth muscle cell differentiation | 2 | 2 | 7.01E-03 |
| Negative regulation of muscle cell differentiation | 2 | 2 | 7.01E-03 |
| Regulation of muscle cell differentiation | 2 | 2 | 7.01E-03 |
| Synaptogenesis | 22 | 7 | 1.63E-03 |
| Synapse organization and biogenesis | 28 | 7 | 7.25E-03 |
| Regulation of cellular process | 3709 | 348 | 7.37E-03 |
| Regulation of biological process | 4009 | 373 | 8.90E-03 |
| Negative regulation of nitric oxide synthase activity | 2 | 2 | 7.01E-03 |
| Negative regulation of oxidoreductase activity | 2 | 2 | 7.01E-03 |
| Antigen processing and presentation of peptide or polysaccharide antigen via MHC class II | 19 | 6 | 3.67E-03 |

| **Molecular Function** | **T** | **R** | **P** |
|---|---|---|---|
| zinc ion binding | 2073 | 226 | 7.10E-05 |
| transition metal ion binding | 2479 | 265 | 5.86E-05 |
| DNA binding | 2025 | 238 | 1.43E-07 |
| nucleic acid binding | 2948 | 326 | 2.00E-07 |
| metal ion binding | 3686 | 366 | 8.20E-04 |
| cation binding | 3416 | 338 | 1.83E-03 |
| ion binding | 3763 | 374 | 6.41E-04 |
| actin binding | 263 | 36 | 3.93E-03 |
| cytoskeletal protein binding | 381 | 17 | 8.33E-03 |
| trans 1,2 dihydrobenzene 1,2 diol dehydrogenase activity | 2 | 2 | 7.48E-03 |
| polyamine oxidase activity | 2 | 2 | 7.48E-03 |
| oxidized purine base lesion DNA N-glycosylase activity | 4 | 3 | 2.42E-03 |
| oxidized base lesion DNA N-glycolase activity | 4 | 3 | 2.42E-03 |
| cGMP inhibited cyclic nucleotide phosphodiesterase activity | 2 | 2 | 7.48E-03 |
| macrophage colony stimulating factor receptor activity | 2 | 2 | 7.48E-03 |
| MHC class II receptor pathway | 15 | 5 | 6.91E-03 |
| gastric inhibitory peptide receptor activity | 2 | 2 | 7.48E-03 |

**Supplemental Table 5** - KEGG pathway analysis results from transient MDA-231 TR microarray experiment.

| z | p value | Description |
|---|---|---|
| -7.94641 | 1.92E-15 | Ribosome |
| -7.75665 | 8.72E-15 | Oxidative phosphorylation |
| -7.71088 | 1.25E-14 | Biosynthesis of steroids |
| -6.58882 | 4.43E-11 | O-Glycan biosynthesis |
| -6.35578 | 2.07E-10 | Apoptosis |
| -6.1325 | 8.65E-10 | Glycan structures - biosynthesis 1 |
| -5.74121 | 9.40E-09 | Pyrimidine metabolism |
| -5.54703 | 2.91E-08 | Ubiquitin mediated proteolysis |
| -5.20739 | 1.92E-07 | One carbon pool by folate |
| -4.94375 | 7.66E-07 | Olfactory transduction |
| -4.80769 | 1.53E-06 | Thiamine metabolism |
| -4.76663 | 1.87E-06 | Synthesis and degradation of ketone bodies |
| -4.76496 | 1.89E-06 | Valine, leucine and isoleucine degradation |
| -4.70202 | 2.58E-06 | Proteasome |
| -4.46983 | 7.83E-06 | mTOR signaling pathway |
| -4.32839 | 1.50E-05 | Insulin signaling pathway |
| -4.29217 | 1.77E-05 | Purine metabolism |
| -4.29038 | 1.78E-05 | Long-term potentiation |
| -4.28458 | 1.83E-05 | Glyoxylate and dicarboxylate metabolism |
| -4.22724 | 2.37E-05 | Type I diabetes mellitus |
| -4.20377 | 2.63E-05 | Terpenoid biosynthesis |
| -3.89974 | 9.63E-05 | Adherens junction |
| -3.76453 | 0.000167 | Butanoate metabolism |
| -3.60239 | 0.000315 | Axon guidance |
| -3.49355 | 0.000477 | Wnt signaling pathway |
| -3.43173 | 0.0006 | ErbB signaling pathway |
| -3.4108 | 0.000648 | Pyruvate metabolism |
| -3.37492 | 0.000738 | Chondroitin sulfate biosynthesis |
| -3.33437 | 0.000855 | Huntington's disease |
| -3.33033 | 0.000867 | Valine, leucine and isoleucine biosynthesis |
| -3.27073 | 0.001073 | Renal cell carcinoma |
| -3.23939 | 0.001198 | Circadian rhythm |
| -3.23367 | 0.001222 | Neurodegenerative Disorders |
| -3.13731 | 0.001705 | Benzoate degradation via CoA ligation |
| -3.08942 | 0.002006 | Sphingolipid metabolism |
| -2.99498 | 0.002745 | Keratan sulfate biosynthesis |
| -2.96183 | 0.003058 | Fructose and mannose metabolism |
| -2.95967 | 0.00308 | Glioma |
| -2.85721 | 0.004274 | Glycan structures - biosynthesis 2 |
| -2.83847 | 0.004533 | Focal adhesion |
| -2.80581 | 0.005019 | Dentatorubropallidoluysian atrophy (DRPLA) |
| -2.7968 | 0.005161 | Nicotinate and nicotinamide metabolism |

| | | |
|---|---|---|
| -2.78528 | 0.005348 | Heparan sulfate biosynthesis |
| -2.7208 | 0.006512 | Glycan structures – degradation |
| -2.68748 | 0.007199 | Gap junction |
| -2.65506 | 0.00793 | Tetrachloroethene degradation |
| -2.62825 | 0.008583 | Phosphatidylinositol signaling system |
| -2.5739 | 0.010056 | Alanine and aspartate metabolism |
| -2.41365 | 0.015794 | Melanoma |
| -2.38859 | 0.016913 | Colorectal cancer |
| -2.37759 | 0.017426 | Tight junction |
| -2.37707 | 0.017451 | Carbon fixation |
| -2.3687 | 0.017851 | Folate biosynthesis |
| -2.23754 | 0.025251 | Bisphenol A degradation |
| -2.16365 | 0.030491 | Methane metabolism |
| -2.14553 | 0.03191 | Starch and sucrose metabolism |
| -2.03595 | 0.041755 | Lysine degradation |
| -2.02022 | 0.043361 | Small cell lung cancer |
| -1.99311 | 0.046249 | ABC transporters – General |
| -1.98024 | 0.047676 | Pantothenate and CoA biosynthesis |
| -1.97359 | 0.048428 | Glycosylphosphatidylinositol(GPI)-anchor biosynthesis |
| -1.87067 | 0.061391 | Regulation of actin cytoskeleton |
| -1.85615 | 0.063432 | Ethylbenzene degradation |
| -1.83891 | 0.065928 | DNA polymerase |
| -1.83152 | 0.067023 | Notch signaling pathway |
| -1.80473 | 0.071117 | Bile acid biosynthesis |
| -1.67647 | 0.093646 | Fatty acid metabolism |
| -1.63483 | 0.102085 | Riboflavin metabolism |
| -1.60175 | 0.109211 | Reductive carboxylate cycle (CO2 fixation) |
| -1.56355 | 0.117923 | Pentose phosphate pathway |
| -1.52965 | 0.126103 | Alzheimer's disease |
| -1.52408 | 0.127489 | Cell adhesion molecules (CAMs) |
| -1.48214 | 0.138304 | Chronic myeloid leukemia |
| -1.46704 | 0.142365 | Antigen processing and presentation |
| -1.44583 | 0.148224 | Methionine metabolism |
| -1.41901 | 0.155895 | Limonene and pinene degradation |
| -1.41508 | 0.157045 | Pancreatic cancer |
| -1.39323 | 0.163551 | Glycosphingolipid biosynthesis – lactoseries |
| -1.38429 | 0.16627 | Inositol phosphate metabolism |
| -1.34804 | 0.177646 | Jak-STAT signaling pathway |
| -1.27556 | 0.202113 | Cell cycle |
| -1.27136 | 0.2036 | Galactose metabolism |
| -1.24997 | 0.211309 | N-Glycan degradation |
| -1.20635 | 0.227681 | 1- and 2-Methylnaphthalene degradation |
| -1.18187 | 0.237257 | Benzoate degradation via hydroxylation |
| -1.08485 | 0.277988 | Glycosphingolipid biosynthesis – globoseries |
| -1.07184 | 0.283791 | Non-small cell lung cancer |
| -1.06552 | 0.286643 | Propanoate metabolism |

| | | |
|---|---|---|
| -1.06001 | 0.289141 | Glycosaminoglycan degradation |
| -0.97814 | 0.328007 | Leukocyte transendothelial migration |
| -0.9713 | 0.331398 | Glutamate metabolism |
| -0.92937 | 0.352696 | Cyanoamino acid metabolism |
| -0.86966 | 0.384487 | Glycolysis / Gluconeogenesis |
| -0.8401 | 0.400853 | Glycerolipid metabolism |
| -0.81339 | 0.415994 | Glycine, serine and threonine metabolism |
| -0.74474 | 0.456429 | Pathogenic Escherichia coli infection – EHEC |
| -0.74474 | 0.456429 | Pathogenic Escherichia coli infection – EPEC |
| -0.72518 | 0.46834 | Phenylpropanoid biosynthesis |
| -0.71616 | 0.473893 | Regulation of autophagy |
| -0.66973 | 0.503029 | Melanogenesis |
| -0.63361 | 0.526332 | Vitamin B6 metabolism |
| -0.6023 | 0.546975 | Sulfur metabolism |
| -0.59391 | 0.552574 | GnRH signaling pathway |
| -0.55687 | 0.577614 | beta-Alanine metabolism |
| -0.4257 | 0.670328 | Amyotrophic lateral sclerosis (ALS) |
| -0.41047 | 0.681462 | Prion disease |
| -0.36319 | 0.716463 | Glycosphingolipid biosynthesis - neo-lactoseries |
| -0.35373 | 0.723543 | Protein export |
| -0.33977 | 0.734028 | Epithelial cell signaling in Helicobacter pylori infection |
| -0.31038 | 0.756275 | Bladder cancer |
| -0.30156 | 0.76299 | Dorso-ventral axis formation |
| -0.30072 | 0.76363 | Toll-like receptor signaling pathway |
| -0.28402 | 0.776392 | Natural killer cell mediated cytotoxicity |
| -0.09647 | 0.923147 | Fatty acid elongation in mitochondria |
| -0.04446 | 0.964536 | Aminoacyl-tRNA biosynthesis |
| 0.004868 | 0.996116 | Nucleotide sugars metabolism |
| 0.042128 | 0.966397 | VEGF signaling pathway |
| 0.099933 | 0.920398 | MAPK signaling pathway |
| 0.118328 | 0.905808 | Aminosugars metabolism |
| 0.151978 | 0.879204 | PPAR signaling pathway |
| 0.173999 | 0.861867 | Acute myeloid leukemia |
| 0.206678 | 0.836261 | C21-Steroid hormone metabolism |
| 0.220249 | 0.825677 | Alkaloid biosynthesis II |
| 0.244632 | 0.806742 | Streptomycin biosynthesis |
| 0.328915 | 0.74222 | Long-term depression |
| 0.356673 | 0.721337 | p53 signaling pathway |
| 0.373629 | 0.70868 | Calcium signaling pathway |
| 0.404926 | 0.685532 | Adipocytokine signaling pathway |
| 0.409938 | 0.681852 | Cholera – Infection |
| 0.440253 | 0.659754 | RNA polymerase |
| 0.457854 | 0.647057 | Basal transcription factors |
| 0.474012 | 0.635491 | gamma-Hexachlorocyclohexane degradation |
| 0.499338 | 0.617541 | Ubiquinone biosynthesis |
| 0.523125 | 0.600887 | B cell receptor signaling pathway |

| | | |
|---|---|---|
| 0.534347 | 0.593101 | Endometrial cancer |
| 0.545953 | 0.585098 | Phenylalanine metabolism |
| 0.552545 | 0.580575 | Glycosphingolipid biosynthesis – ganglioseries |
| 0.554004 | 0.579576 | Ascorbate and aldarate metabolism |
| 0.658538 | 0.510192 | Type II diabetes mellitus |
| 0.72325 | 0.469527 | Basal cell carcinoma |
| 0.866201 | 0.38638 | T cell receptor signaling pathway |
| 0.891546 | 0.372636 | Urea cycle and metabolism of amino groups |
| 0.925765 | 0.354568 | Glutathione metabolism |
| 1.009307 | 0.312827 | Fc epsilon RI signaling pathway |
| 1.014032 | 0.310567 | Thyroid cancer |
| 1.035254 | 0.30055 | Selenoamino acid metabolism |
| 1.132198 | 0.257551 | SNARE interactions in vesicular transport |
| 1.144238 | 0.252525 | TGF-beta signaling pathway |
| 1.213972 | 0.224758 | Hematopoietic cell lineage |
| 1.240353 | 0.214845 | Caprolactam degradation |
| 1.276691 | 0.201711 | Prostate cancer |
| 1.413849 | 0.157406 | Hedgehog signaling pathway |
| 1.438455 | 0.150305 | Glycerophospholipid metabolism |
| 1.457693 | 0.144925 | Parkinson's disease |
| 1.459738 | 0.144362 | Cysteine metabolism |
| 1.640367 | 0.100929 | 2,4-Dichlorobenzoate degradation |
| 1.78364 | 0.074482 | Linoleic acid metabolism |
| 1.810873 | 0.070161 | Tryptophan metabolism |
| 1.91878 | 0.055012 | Citrate cycle (TCA cycle) |
| 1.92259 | 0.054532 | Arginine and proline metabolism |
| 1.935078 | 0.052981 | Aminophosphonate metabolism |
| 2.114271 | 0.034492 | Nitrogen metabolism |
| 2.114302 | 0.034489 | Naphthalene and anthracene degradation |
| 2.173186 | 0.029766 | Ether lipid metabolism |
| 2.329344 | 0.019841 | Taurine and hypotaurine metabolism |
| 2.349429 | 0.018802 | Renin-angiotensin system |
| 2.353877 | 0.018579 | Alkaloid biosynthesis I |
| 2.436073 | 0.014848 | Pentose and glucuronate interconversions |
| 2.47494 | 0.013326 | ECM-receptor interaction |
| 2.580341 | 0.00987 | N-Glycan biosynthesis |
| 2.608033 | 0.009106 | Histidine metabolism |
| 2.927623 | 0.003416 | Complement and coagulation cascades |
| 3.05579 | 0.002245 | Phenylalanine, tyrosine and tryptophan biosynthesis |
| 3.095907 | 0.001962 | Cytokine-cytokine receptor interaction |
| 3.110163 | 0.00187 | Taste transduction |
| 3.179501 | 0.001475 | Tyrosine metabolism |
| 3.494923 | 0.000474 | Atrazine degradation |
| 3.85381 | 0.000116 | Fatty acid biosynthesis |
| 4.173509 | 3.00E-05 | Arachidonic acid metabolism |
| 4.724546 | 2.31E-06 | Metabolism of xenobiotics by cytochrome P450 |

| | | |
|---|---|---|
| 4.824256 | 1.41E-06 | Maturity onset diabetes of the young |
| 5.050351 | 4.41E-07 | Cell Communication |

Appendix 2 - Ductal outgrowth delay in MMTV/CrkI and MMTV/CrkII transgenic mice, but not in MMTV/CrkLV5 or FVB mice.